ResearchGate

See discussions, stats, and author profiles for this publication at: https://www.researchgate.net/publication/226007454

Another look at nagyágite from the type locality, Scrîmb, Romania: Replacement, chemical variation and petrogenetic implications

Article *in* Mineralogy and Petrology · January 2008

DOI: 10.1007/s00710-007-0220-6

CITATIONS
21

READS
171

5 authors, including:

Cristiana L. Ciobanu
University of Adelaide
147 PUBLICATIONS 2,496 CITATIONS

SEE PROFILE

Nigel J Cook
University of Adelaide
231 PUBLICATIONS 3,744 CITATIONS

SEE PROFILE

Allan Pring
Flinders University
281 PUBLICATIONS 3,226 CITATIONS

SEE PROFILE

Gheorghe Damian
North University Center of Baia Mare, Technical University of Cluj ...
57 PUBLICATIONS 449 CITATIONS

SEE PROFILE

Some of the authors of this publication are also working on these related projects:

Project Telluride and selenide minerals View project

Project Meteorites View project

All content following this page was uploaded by Cristiana L. Ciobanu on 01 June 2014.

The user has requested enhancement of the downloaded file.

Mineral Petrol (2008) 93: 273–307
DOI 10.1007/s00710-007-0220-6
Printed in The Netherlands

Mineralogy and Petrology

Another look at nagyágite from the type locality, Săcărîmb, Romania: Replacement, chemical variation and petrogenetic implications

C. L. Ciobanu[1,2], N. J. Cook[3], A. Pring[1,2], G. Damian[4], N. Căpraru[5]

[1] Department of Mineralogy, South Australian Museum, Adelaide, Australia
[2] Department of Earth and Environmental Sciences, University of Adelaide, Adelaide, Australia
[3] Natural History Museum, University of Oslo, Oslo, Norway
[4] North University of Baia Mare, Baia Mare, Romania
[5] Speranţa Str. 3, Dezna, Arad, Romania

Received May 4 2007; revised version accepted October 3 2007; Published online December 6 2007
© Springer-Verlag 2007
Editorial handling: P. Spry

Summary

Extensive compositional heterogeneity is displayed by Pb-Sb-Au tellurides from the type locality at Săcărîmb. These phases are collectively considered as varieties of nagyágite in the absence of crystal chemical data confirming the presence of distinct, but topologically closely related compounds. Chemical heterogeneity is seen relative to 'normal' nagyágite, with close to the ideal composition $Pb_3[Pb_{1.8}(Sb_{1.1},As_{0.1})_{1.2}]_{\Sigma 3}S_6(AuTe_2)$, which is the primary and common type in the deposit. A modified formula, $(Pb_3S_3)[(Pb_{2-x})(Sb,As,Te_b)_{1+x}(S_{3-y}Te_y)]_{\Sigma 6}(Au_{1-z-w}Te_{2+z}S_w)$, accounts for the chemical variation observed. Values of x (0.2 to 1.15) express substitution of Pb by Sb + As for Me_2 in sulfosalt modules in the case of Au-depleted and low-Au nagyágite, and by Sb + As + Te_b in high-As and low-Pb varieties ($b = x + 1 - (Sb + As) = 0.24$ to 0.29). Excess Te compensates for Au deficiency in the telluride layer, with substitution by S also observed; empirical values of z and w are 0 to 0.45 and 0 to 0.32, respectively. Minor substitution of Te for S ($y < 0.17$) is noted in all varieties except low-Au.

Correspondence: C.L. Ciobanu, South Australian Museum, North Terrace, Adelaide, SA 5005, Australia
e-mail: Cristiana.Ciobanu@adelaide.edu.au; Ciobanu.Cristiana@saugov.sa.gov.au

These varieties are formed during replacement of the 'normal' type as seen in overprinting relationships in those veins reactivated during rotation of the duplex fault-system responsible for vein formation. Replacement is by coupled dissolution-reprecipitation reactions, as indicated by pseudomorphism of one nagyágite type by another in all cases. Variable rates of both molar-excess and -deficit reaction are invoked to explain the observed chemical and textural modifications. Low-Pb nagyágite is also present in zoned platelets where it grows over resorbed cores of ideal composition. Such platelets are instead interpreted as products of self-patterning in a residual precipitate. A marked depletion in the Au content of some nagyágite lamellae is considered to be a diffusion driven Te for Au substitution in the presence of Te-bearing fluid.

Replacement of 'normal' nagyágite by other varieties can be linked to high fluid acidity, whereas replacement by galena-altaite symplectites relates to changes in the fTe_2/fS_2 within a narrow domain defined by coexistence of these two minerals. Nagyágite is a mineral with modular crystal chemistry and is able to adjust to variable rates of fluid infiltration by subtle chemical substitutions. The behavior of nagyágite will map and assist coupling between dissolution and precipitation during such reactions.

Introduction

The Săcărîmb deposit, in the Golden Quadrilateral, South Apuseni Mts., Western Romania, is the type locality for several gold and silver telluride species (krennerite, petzite, stützite, nagyágite, muthmannite, museumite). This is one of several gold-telluride deposits worldwide that consists of veins formed in an epithermal environment, which at Săcărîmb are of low-sulfidation type (Berbeleac et al., 1995). The mineralization is related to Neogene calc-alkaline magmatism. Cook and Ciobanu (2005) have drawn attention to the fact that this is a good, though not unique, example of a deposit that contradicts the widely-held opinion that gold-telluride deposits display an alkaline affiliation (Jensen and Barton, 2000).

The complex Pb-Sb-Au sulfotelluride nagyágite, one of the main components in the exploited ore, is named for the deposit, Nagyág being the Hungarian name of the village and associated mines at the time the deposit was discovered. High-grade telluride ore formed the basis of exploitation of the deposit from the 1770's until its closure in 1991. Historical production figures infer that Săcărîmb produced 32 tonnes of Au and 50 tonnes of Ag since its discovery (Udubaşa et al., 1992).

Nagyágite was first mentioned by Scopoli (1769) as *minera aurifera Nagyagensis* and was named by Haidinger (1845); see Papp (2004) for a detailed account of the early history of nagyágite. Since its discovery, considerable efforts have been devoted to determine the compositional limits and formula of nagyágite (Schrauf, 1878; Sipöcz, 1885; Hankó, 1888; Helke, 1934; Gossner, 1935; Giuşcă, 1937; Stumpfl, 1970; Udubaşa, 1986; Spiridonov, 1991; Udubaşa et al., 1993; Stanley et al., 1994; Lupulescu, 1997). Despite an early belief that nagyágite was essentially stoichiometric (e.g., Stumpfl, 1970), compositional heterogeneity was noted by several authors for nagyágite from Săcărîmb (Giuşcă, 1937; Udubaşa, 1986; Cioflica et al., 1993a; Şimon et al., 1994; Stanley et al., 1994; Lupulescu, 1997). The last three contributions demonstrated that there is significant substitution of Sb by As, coupled to Pb deficiency, as well as variation in the $Au/(Au + Te)$ ratio. Similar trends were also noted more recently by Shimizu and Stanley (2003).

The structural formula of nagyágite: $[Pb(Pb,Sb)S_2][(Au,Te)]$, $Z = 2$, was determined by Effenberger et al. (1999) who report a monoclinic parent cell in space group $P2_1/m$ with $a = 4.220(1)$, $b = 4.176(1)$ $c = 15.119(3)$Å and $\beta = 95.42(3)°$. The structure is an ordered intergrowth of two types of layers: (i) (Pb,Sb)S–a sulfosalt layer, and (ii) (Au,Te)-telluride (T) that are stacked along the c axis. Four sulfosalt layers are combined into two slabs with tetragonal SnS-like motif (Q) (Makovicky, 1993). In the parent structure the Q slab contains 2 metal positions of which one (Me_1), is fixed by structural refinement as a Pb-only site. The other (Me_2) is a mixed site in which Me^{2+} (Pb) or Me^{3+} (Sb, As, Bi) can be incorporated. The T layer features a square net in which Au and Te are assigned to a single crystallographic position, although the two elements are considered unlikely to form a solid-solution. Effenberger et al. (1999) postulate that Au^{3+} has a 4-fold planar coordination with Te and such squares are connected by edges into chains; Te atoms form a zig-zag arrangement between the Au chains. This configuration is based on an assumed ideal ratio Au:Te = 1:2 and the often observed tripling of one of the short axes (**a** or **b**).

The tripled cell parameter in nagyágite corresponds to b parameter in the related sulfotelluride, buckhornite: $[(Pb_2Bi)_{\Sigma 3}S_3][(Au,Te_2)_3]$, ($Z = 2$) (Effenberger et al., 2000). The two minerals are part of the nagyágite series in which the number of Q modules between T layers defines the homologue number (N). The homology becomes apparent when the nagyágite formula is rewritten for the triple average cell ($b_{buckhornite} \sim 3 \times b_{nagyágite}$) as $[Pb_3(Pb,Sb)_3S_6][(Au,Te)_3]$ ($Z = 2$), showing that nagyágite and buckhornite are the $N = 2$ and $N = 1$ members, respectively. Museumite, $[Pb_2(Pb,Sb)S_8](Te,Au)_2$, is discussed as a structurally related mineral (Bindi and Cipriani, 2004).

In nagyágite, the most common ratio of Pb to Sb in the Me_2 site found in nature seems to be close to 2:1 and the ratio of Au to Te is close to 1:2 for the tripled average cell. The structure and composition of the sulfosalt layer seems to have much in common with other layered complex sulfides such as franckeite and $[(Pb,Sb)S]_{2.28}NbS_2$ which also show a preferred Pb:Sb ratio in the Me_2 site, in this case 3:2 (Bengel et al., 2000). In the full $3 \times \mathbf{a}(\mathbf{b})$ super cell the single Me_2 site will, by symmetry considerations, be split into a number of crystallographically distinct sites. Preliminary electron microscopy and electron diffraction studies by us confirm the basic subcell reported by Effenberger et al. (1999) but note a range of complex supercells/modulations with ordering along either **a** and **b** depending upon the chemistry of nagyágite.

The compositions of nagyágite from other localities that represent either epithermal (e.g., Cripple Creek, USA; Stumpfl, 1970; Eckel, 1997), or metamorphic environments (e.g., Schellgaden, Austria; Paar and Chen, 1982), Sunrise Dam, Western Australia (Sung et al., 2007) are all close to an ideal formula: $[(Pb_3(Pb_{1.8}Sb_{1.2})S_6][AuTe_2]$. Thus, this appears to be the most common and stable variety of nagyágite, also present at Săcărîmb.

What is the range of nagyágite composition at Săcărîmb and what drives this variability? This is the subject of the present paper, attractive not only for establishing the compositional limits for nagyágite, but also for understanding their stabilities in a hydrothermal system. In a previous study on samples from Săcărîmb, Ciobanu et al. (2004a) documented (i) exchange of As for Sb, (ii) variation in

the Au/(Au + Te) ratio, and (iii) variation in the Pb/(Pb + Sb + As) ratio that is independent of As/(As + Sb). The present contribution extends this earlier dataset (which was based exclusively on analyses by SEM-EDS), using electron probe microanalysis to quantify the extent of the three exchanges above, and the inferences this may have for characterization of nagyágite. Secondly, this compositional variation is seen in connection with a range of textures that deserves attention for their petrogenetic implications at Săcărîmb or elsewhere.

The Săcărîmb deposit

Geodynamic setting

Săcărîmb is the southernmost among 32 known deposits/prospects in the easternmost and longest tectono-magmatic alignment in the Golden Quadrilateral, i.e., Brad-Săcărîmb (Fig. 1a). Drew (2003) considered that the opening of troughs hosting magmatic activity was along NW–SE faults during a 17–15 Ma (Early to Middle Miocene) extensional regime and followed a pre-existing anisotropy inherited from the Jurassic basement; this in turn controlled the position of extensional stepovers in the smaller basins within each trough. Such repartition is realized during the change from an initial pull-apart regime to later strike-slip tectonics (Middle to Late Miocene), followed by emplacement of volcanic rocks and intrusions (mainly andesitic) in extensional stepovers. Săcărîmb is positioned at the SE end of the Săcărîmb-Hondol-Bolcana district, in which porphyry stocks and vein meshes are not associated with one another within the same deposit, as in other districts in the Golden Quadrilateral (e.g., Zlatna-Stănija, Brad). This is interpreted as a function of the regional evolution of this area, in which the duplex-system is formed by master faults underlying the margins of the trough (Drew, 2003), with Săcărîmb representing one of the more complex extensional stepovers. This approach offers a unitary model for mineralizing styles in the Golden Quadrilateral, even though whether the onset of the requisite tectonic setting for magmatism occurred during the Neogene, as Drew assumes, and not earlier is debatable (see Ciobanu et al., 2004b).

Vein characteristics

Most of the 230 veins that make up the deposit (Helke, 1934; Giuşcă, 1935, 1936a, b; Ianovici et al., 1976) are located within a small area (1 km^2) of an andesitic stock with central position in a volcanic edifice (Central Neck; Fig. 1b). The entire structure is emplaced close to the intersection of NW–SE and E–W fracture systems, which form the boundaries of the basin towards the basement rocks (Fig. 1a). Pálfy (1912) was the first to note the branched and funnel-shaped morphology of the Central Neck, with blocks of country rocks displaced and melded within the neck during ascension of magma (Fig. 1b). Căpraru (2004) interprets such relationships as evidence for subsidence-collapse with probable evolution to a diatreme ± maar stage for the Central Neck that also features a radial relationship with the satellite volcanic centers and a tendency to a marginal segregation following fractures and ring/curviplanar faults (Fig. 2).

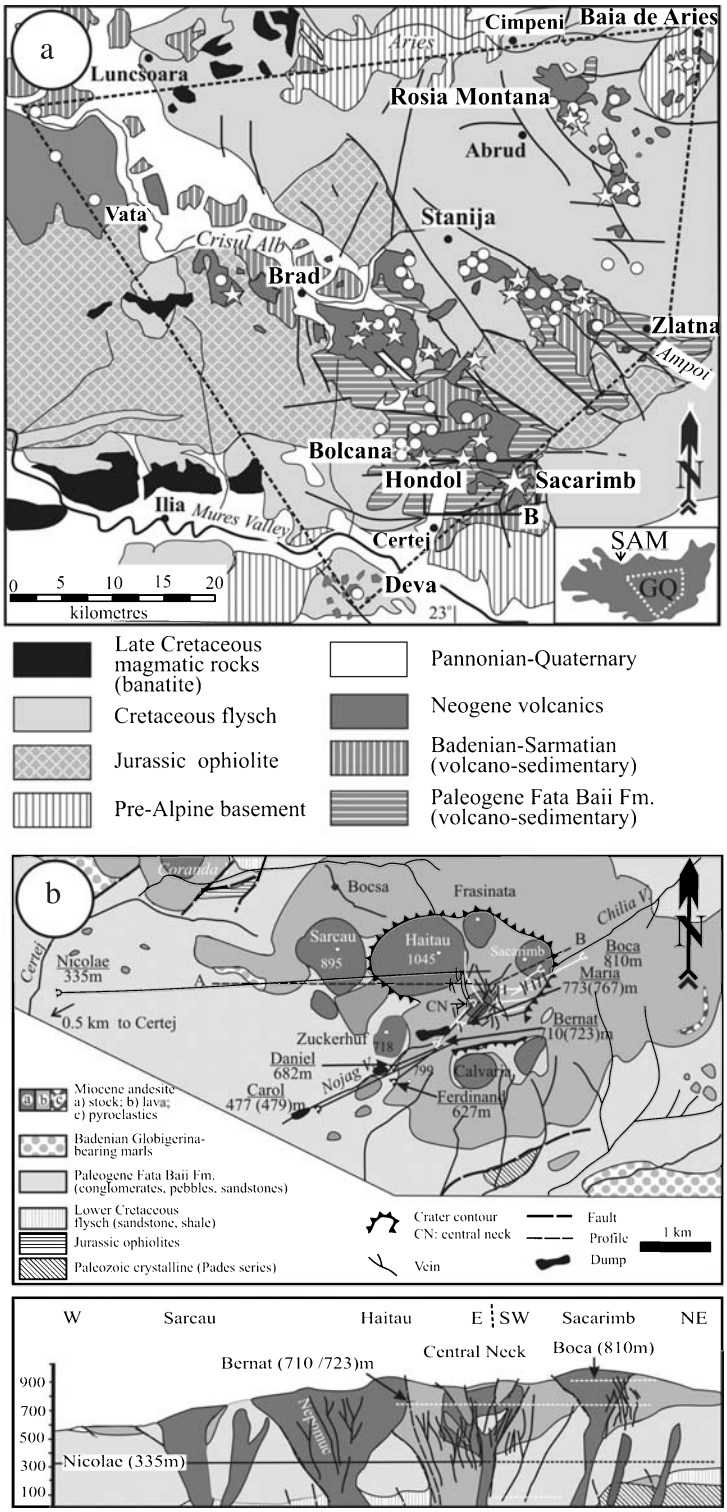

Fig. 1. (**a**) Geological map of the Golden Quadrilateral (GQ) in Romania, showing the location of Săcărîmb deposit. Inset shows position of the Golden Quadrilateral within the South Apuseni Mts. (SAM) of W Romania. Open circles: Au deposits; Open stars: telluride occurrences in Au deposits. (**b**) Geological map and cross section (A-B) of Săcărîmb orefield. (Numbers in brackets indicate gallery levels in old topographic system). Sources of original maps are given by Ciobanu et al. (2004b)

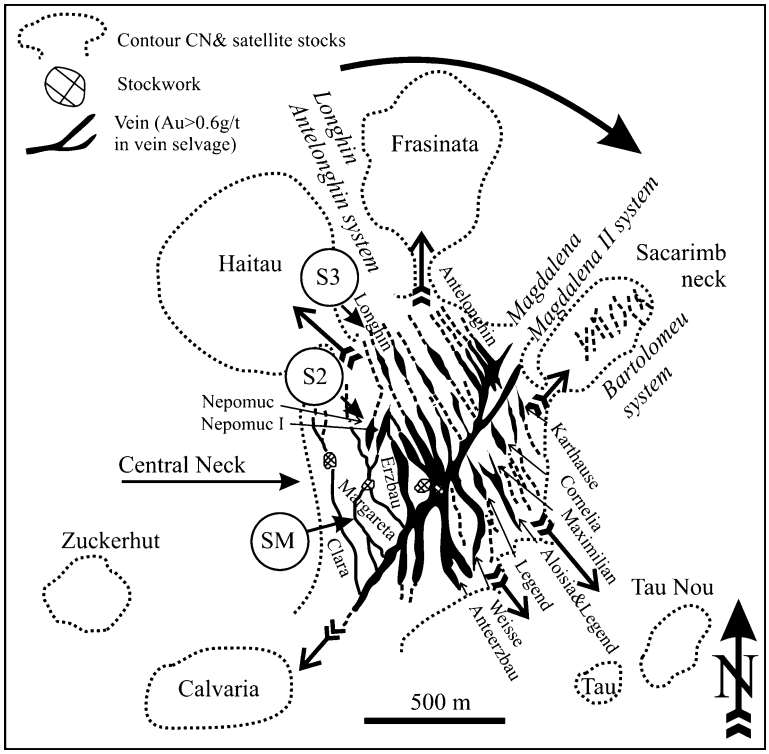

Fig. 2. Position of vein systems on the Bernat level (710 m), as remapped during re-evaluation by Deva Gold SA in 2004. The Central Neck (CN) and satellite stocks are shown in projection. Arrows with double tail show direction of lava flow between the Central Neck and surrounding stocks. Simple arrows indicate sense of rotation during vein opening, controlled by the evolution of the regional duplex-system (Drew, 2003). Allocation of samples to individual vein systems is shown as circles. Although samples are from deeper levels than Bernat (accessible only during mine operation), the relative positions of the vein systems remain the same

The veins form a dense mesh and they are steep, with a vertical extension of some 400–600 m and lengths of <100–150 m at upper levels and >400 m (e.g., Magdalena) in the median part; the average width is ca. 30 cm although this may vary from several cm to 2 m within pinch and swell structures along strike. The entire mineralized zone has a vertical plunge and is known from underground mines between levels 810 m (Boca) and 135 m (Fig. 1b); maximum extension of veins is attained between the levels Ferdinand (627 m) and Carol (477 m). Căpraru (2004) noted that most of the veins are clustered in parallel systems with crosscutting relationships, which he interpreted in relation with transposition of a strike-slip duplex fault system, from NW–SE to E–W (Fig. 2), in response to the regional evolution of the area.

Ore assemblages and their distribution

In their overview of deposits in the Golden Quadrilateral, Ghiţulescu and Socolescu (1941) give the following exploitation record of gold speciation and distribution in the three main vein systems at Săcărîmb: (i) nagyágite in Magdalena; (ii) sylvanite

and native Au, rare nagyágite in Longhin; (iii) sylvanite and petzite in Nepomuc (see Fig. 2). Unlike any other deposit in the Golden Quadrilateral, in Săcărîmb the veins contained a dominance of Au-(Ag)-tellurides over native gold, which is maintained throughout the high-grade middle part of deposit (Cook et al., 2004). Native gold was exploited mainly from low-grade, sulfide-sulfosalt ore (scarce tellurides) at uppermost levels. This represents an inverse zonation trend compared to other deposits in the Golden Quadrilateral (Udubaşa et al., 1992) or elsewhere (Cooke and McPhail, 2001).

Nagyágite is one of 22 telluride species reported from the deposit. The telluride suite includes a wide variety of Au-(Ag)-tellurides, other tellurides, i.e., altaite, tellurantimony, coloradoite, frohbergite (see Cook et al., 2004 and references therein) and several Bi-(Pb)-tellurides (Şimon and Alderton, 1995; Shimizu et al., 1999; Cook et al., 2005). Ciobanu et al. (2004a) gave a contemporary overview on tellurides and sulfosalts from the veins at Săcărîmb, discussing their speciation and phase relationships. Based on these data, telluride formation was estimated at 290–300 °C. Abundant As-Sb-sulfosalts (mainly from the bournonite-seligmannite and jordanite-geochronite series) and rare Bi-sulfosalts are co-genetic with tellurides in the margins of the vein (*salband*) (Ciobanu et al., 2005), whereas replacement is typical for the filling of the same vein.

Nagyágite was widely present at Săcărîmb and is typical for the Magdalena veins. Although less common, the association of nagyágite with rhodochrosite and alabandite is characteristic for the Longhin vein system. As-nagyágite (Şimon et al., 1994) is considered to have been from the Nepomuc vein. Lupulescu (1997) contends that Au-poor/Te-rich nagyágite was deposited after sylvanite and hessite. Increasing a_{As} in the latter part of the crystallization sequence is indicated by the increasing As content of co-existing bournonite and late deposition of native arsenic on nagyágite crystals.

Fluid characteristics and genetic interpretation

Alderton et al. (1997) reported homogenization temperatures (T_h) of around 260–300 °C and low salinities of 1–4 wt.% eq. NaCl from vein quartz at Săcărîmb. Their conclusion was that evidence for boiling is uncommon for the main stage telluride-mineralization; this is, however, reported from fluid inclusions in quartz from the upper parts of veins (Bernat level; 710 m) (Gál et al., 2003). Stable (C, O, H) isotope evidence from the Săcărîmb area points to a single ore-forming event, with Au, Ag, Te, base metals, S and C derived directly from a crystallizing magma and only a negligible input from meteoric waters (Alderton et al., 1997; Alderton and Fallick, 2000).

Based upon evidence of ore deformation and abundance of pinch-and-swell structures, Ciobanu et al. (2004a) argued that sustained throttling prompted by activation of the duplex faults centered on the Central Neck assisted ore deposition. Moreover, pressure variation (associated with throttling) would have been enhanced along strike rather than plunge given the fact that the Central Neck was most likely buried under volcanic rocks/sediments at the time of vein opening. If so, the epithermal system would not be connected with surficial fractures at the top, a fact that could explain also the lack of mixing between magmatic and meteoric waters as mentioned above. This may also explain the inverse zonation, since the

model of Cooke and McPhail (2001) assumes upward migration of Te vapors after their separation from fluids, due to processes such as boiling; at Săcărîmb, Te condensation is controlled by tectonic-assisted pressure variation at depth.

Sample description and textural relations of nagyágite

In this paper, we focus on three samples from the collection at Baia Mare University that are representative of the range of chemical composition for nagyágite. They were collected from (i) Nepomuc (S2), (ii) Longhin (S3) and (iii) Margareta (SM) veins (Fig. 2). Longhin is one of the major veins with NW-trending direction, perpendicular to Magdalena (NE-trending), whereas Nepomuc and Margareta (to the SW) are branching veins between Longhin and Magdalena (Fig. 2). Although we do not know the exact location of the samples, these veins are all situated on the western side of Magdalena, whereas Longhin is at the northern and Margareta at the southern side; Nepomuc is positioned between them. Tellurides in the samples (Table 1), in which nagyágite is a main component, occur as elongated lamellae within quartz and/or carbonate gangue; sulfides are scarce. There is little difference in terms of the telluride species encountered in each sample although these differ in relative proportions (e.g., petzite is more abundant than sylvanite in sample SM). Another marked difference is that rhodochrosite is the major gangue mineral in sample S3, whereas quartz and/or calcite are prominent in the others. Nagyágite, with a composition close to 'ideal', as discussed above, and which we call 'normal' at Săcărîmb, is present in all samples as thin lamellae, several mm to 1 cm long (attained in S3), with random orientation. This normal nagyágite is overprinted by a later replacement generation. The replacement style, even though it differs from one sample to another, both in terms of the resulting mineral associations and textures (see below), preserves the lamellar shape of nagyágite (pseudomorphs). Although compositional trends in nagyágite will be quantitatively documented in the following section, they are nonetheless introduced here since they appear to be strongly linked to textural development.

Sample S3-Longhin vein

The nagyágite lamellae appear single or in bundles and display a characteristic jigsaw or sawtooth boundary (depending upon the orientation of carbonate rhombohedra) marked irregularly by a rim of altaite towards the host rhodochrosite; the latter is enriched in Mg along the contact. Many of the lamellae are replaced by symplectites of altaite and galena (Fig. 3a). Such symplectites are typical of breakdown textures since the two elements in the intergrown minerals account for the bulk of nagyágite composition. The symplectitic areas follow deep inliers parallel to the lamellae elongation; some lamellae are completely replaced by the symplectites. Galena was observed alone in some of the lamellae and its morphology mimics that of the nagyágite. Overall, the textures above indicate that nagyágite has been pseudomorphosed, in variable proportions in individual lamella, either by breakdown galena-altaite symplectites or by galena.

Semseyite is an additional, yet minor, component in or around the breakdown areas, either as symplectites with altaite (Fig. 3b) or selvages along the replacement

Table 1. *Summary of minerals present in the 3 samples*

Mineral	Sample		
	S3	S2	SM
nagyágite	X	X	X
sylvanite	X	X	X
krennerite	x		X
petzite	x		X
hessite	x	x	X
stützite	x		x
altaite	x	x	X
tellurantimony	x	x	X
coloradoite	x	x	X
*unnamed $(Ag,Au)_2AsTe_2$	x		
native gold	x		
native tellurium	x		
dufrénoysite $[Pb(Sb,As)_2S_4]$		x	
jordanite-geocronite	x	x	
guettardite $[Pb_2(Sb,As)_2S_5]$	x		
stibnite		x	
semseyite	x		
bournonite-seligmannite	X	X	X
tetrahedrite-tennantite		x	
galena	x	x	X
sphalerite	x		X
alabandite	x		
pyrite	x	x	X
arsenopyrite			X
**Te-bearing löllingite	x		
chalcopyrite	x	x	
marcasite		x	x
quartz	x	X	X
rhodochrosite/kutnahorite	X	x	x
other carbonates	x	x	x
Sericite	x	x	x

'X' indicates main component, 'x' represents a minor component

* Unnamed Ag-Au-As telluride: mean of 4 analyses, wt.% Ag 35.34, Au 7.64. Sb 0.31, As 12.62, Te 45.19, Se 0.10, Total 101.19. Empirical formula: $(Ag_{1.83}Au_{0.22})_{\Sigma 2.05}(As_{0.94}Sb_{0.01})_{\Sigma 0.95}(Te_{1.99}Se_{0.01})_{\Sigma 2}$

** Te-bearing löllingite: mean of 4 analyses, wt.%, Ag 0.67, Fe 25.07, Bi 0.07, Sb 0.20, As 58.94, Te 11.56, Se 0.59, S 1.70, Total 98.95. Empirical formula: $(Fe_{0.98}Ag_{0.01})_{\Sigma 0.99}(As_{1.71}Te_{0.20}S_{0.09}Se_{0.02})_{\Sigma 2.01}$

boundary (Fig. 3c). Nagyágite lamellae that are partially replaced by symplectites are revealed as darker zones in the back-scattered electron images (BSE) and correspond to a lower Au content (0.7 apfu, considering 15 apfu, see below; Fig. 3c). Other minerals, such as hessite and native tellurium, occur as inclusions

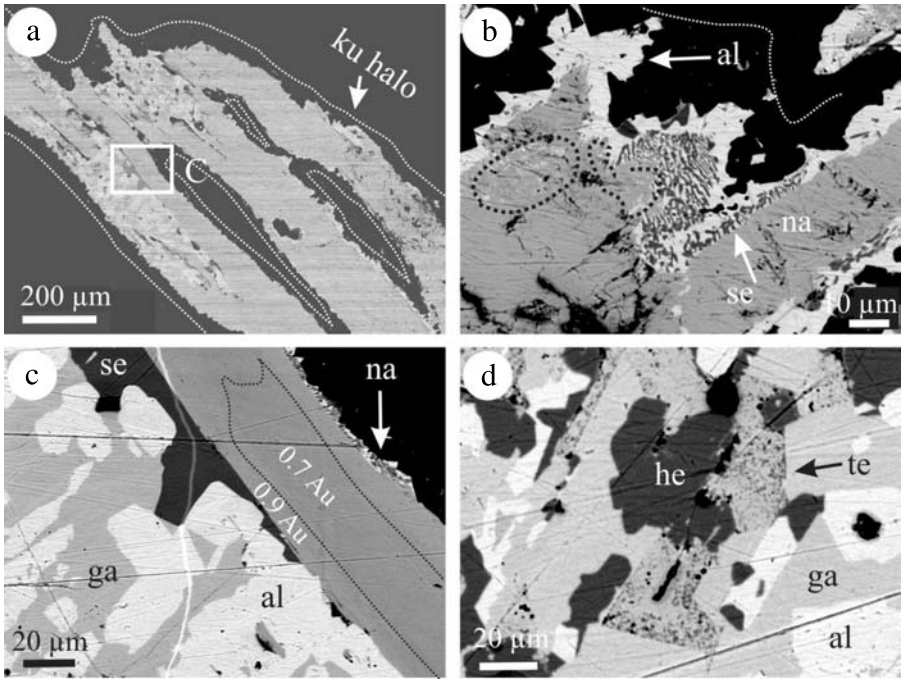

Fig. 3. Back-scattered electron images of nagyágite in sample S3 (Longhin vein). (**a**) Replacement of nagyágite lamellae by symplectites of galena and altaite typical for molar-excess reaction. (**b**) Altaite rim and symplectites of semseyite and altaite along the margin of nagyágite lamella. (**c**) Detail of symplectites in (**a**) showing semseyite sealing the contact towards the adjacent nagyágite lamellae. Note darker shades along this lamella that correspond to Au-depleted portions. (**d**) Inclusions of hessite and native tellurium in the galena-altaite symplectites. Note the porosity of native tellurium. *al* altaite; *ga* galena; *he* hessite; *ku* kutnohorite; *se* semseyite; *te* native tellurium

in some of the areas of decomposition (Fig. 3d). In such instances, we note the relatively high porosity of these areas in and around the fine-grained aggregates of native tellurium. Native gold was observed as tiny inclusions (Fig. 4a) or coarser grains (Fig. 4b) in the carbonate halos seen around lamellae that have been completely replaced by galena. Such halos, clustered by inclusions containing minerals from the lamella they surround, are present even when the nagyágite is not affected by replacement. The halos are seen either with margins preserving the nagyágite shape (pseudomorphosis; Fig. 4a) or irregular (Fig. 4b); the latter is associated with corrosion and advanced replacement of nagyágite.

Sample S2 – Nepomuc vein

Fracture assisted brecciation (Fig. 5a) is observed throughout sample S2. There are at least two sets of veinlets, with Mg-carbonate in the latest, which affected both the host carbonate-quartz gangue and the telluride (nagyágite and sylvanite) lamellae. Nagyágite also features symplectites, but these differ from those in S3 in that they surround, rather than intrude individual lamellae (Fig. 5b). Secondly, they are formed by altaite and a variety of nagyágite that appears darker in BSE images

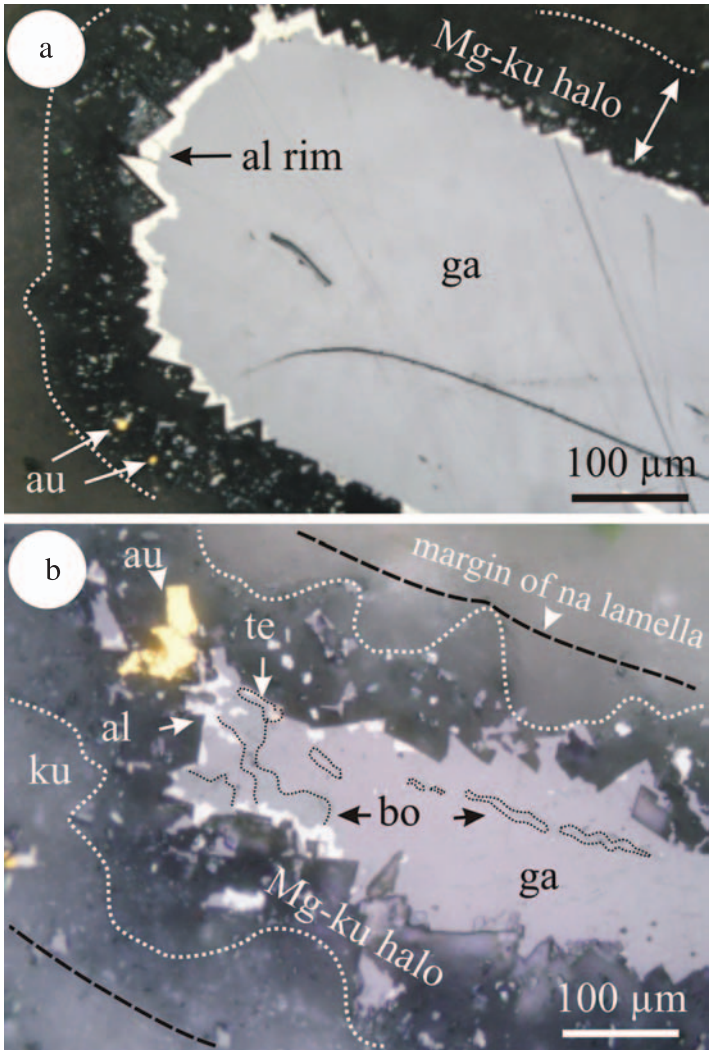

Fig. 4. Photomicrographs of sample S3 (Longhin vein) showing occurrence of native gold in the carbonate halos around nagyágite completely replaced by galena (pseudomorphosis). (**a**) Dusty gold in a halo that has a jigsaw and sawtooth contact (stepwise replacement interface) towards the parent lamella typical for molar deficit reaction; the front is sealed by an altaite rim. Note also inclusions of galena and altaite within the halo. (**b**) Coarse-grained gold in a halo that becomes irregular relative to the original margin of nagyágite. The replacement interface is also irregular, indicating that there is no longer a coupling between dissolution and precipitation. Note the occurrence of native tellurium in the same halo with native gold. Abbreviations are the same as in Fig. 3; *au* native gold; *bo* bournonite-seligmannite; *rh* rhodochrosite

rather than galena. The nagyágite in the symplectites has a higher, but variable, As content than the lamella core; the latter has also lower Au content than the rim (i.e., average 0.65 and 0.83 apfu, respectively).

Other lamellae, especially where crosscut by veinlets of bournonite, show replacement textures that are more complex. One such lamella (Fig. 5c) consists of larger masses of altaite and bournonite along its margin; in between these two is a

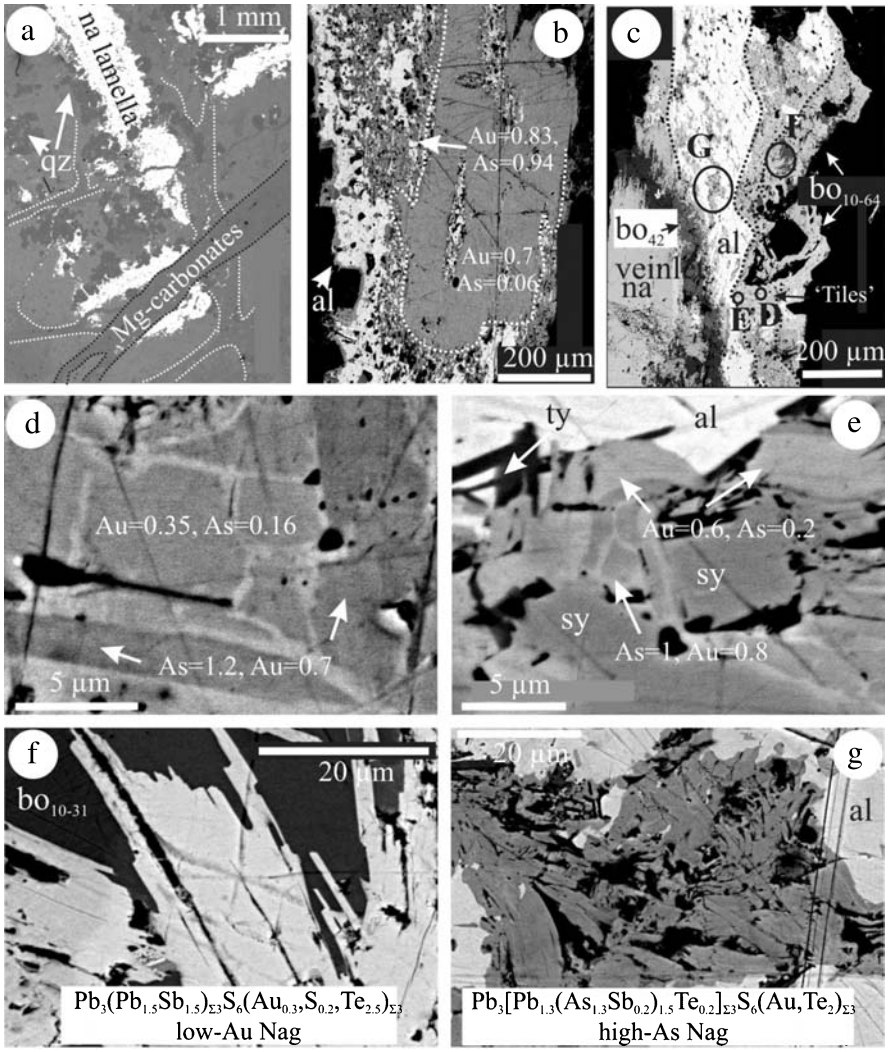

Fig. 5. Back-scattered electron images of sample S2 (Nepomuc vein). (**a**) Two sets of post-telluride-deposition fractures; Mg-carbonate fills the latest generation. (**b**) Halo of symplectites with altaite and high-As nagyágite (darker shades) surrounding a nagyágite lamella; note that the Au content is 0.7 apfu, lower than the ideal value (1 apfu), indicating the same Au-depletion as in sample S3. (**c**) Different mineral replacement zones at the edge of a nagyágite lamella; altaite, nagyágite with changed composition ('tiles') and bournonite; note also the bournonite veinlet crosscutting the same lamella. (**d**, **e**) Details on the tiles areas where nagyágite shows two different compositions (i) low-Au and (ii) high-As. Relict nagyágite is present as a web-like network of lighter color in the image and the other nagyágite varieties are darker. Note, in e, the bending of the nagyágite lamella around the sylvanite grain, taken as evidence for a volume increase reaction during sylvanite growth. (**f**) Low-Au nagyágite in bournonite (**g**) High-As nagyágite nested within altaite. Abbreviations are the same as in Figs. 3 and 4; *qz* quartz; *sy* sylvanite; *ty* tellurantimony. Compositional data for bournonite-seligmannite (e.g., bo_{42}) indicate mol.% bournonite within the bournonite-seligmannite solid solution series

mass of decomposed nagyágite, with a distinctive 'tiled' appearance (Fig. 4d, e), interspersed by rounded or scalloped grains of Ag-rich (Ag:Au ~ 1) sylvanite. The latter differs from the sylvanite that occurs as discrete lamellae in the sample; these are not Ag-rich (Ag:Au ~ 0.3). The tiles (<5 μm in size) appear in BSE images as a web-like net of lighter color (relict nagyágite) within a darker background, which consists either of nagyágite that is low in Au content (0.35 apfu Au; Fig. 5d) or high in As (Fig. 5e). The two varieties are found together in such areas, although the tiled texture is only seen in one phase at a time. Bent crystals of nagyágite occur between altaite and sylvanite.

Bladed aggregates of nagyágite with various orientations occur within bournonite, which surrounds the nagyágite lamellae affected by overprinting (Fig. 5f); these aggregates have a consistently low-Au content (0.3 apfu Au). Their smaller size and different orientations compared to the main nagyágite lamellae (e.g., perpendicular in Fig. 5f), is evidence that such crystals are products of a distinct crystallization process. The same is apparent for flaky, deformed and porous aggregates of nagyágite that are nested within the altaite that replaced the same lamella (Fig. 5g). These aggregates represent a nagyágite variety that has the highest As-content (1.48 apfu As), lowest Sb-content (e.g., 0.1 apfu Sb) and highest Au-content (e.g., 0.94 apfu Au).

Sample SM-Margareta vein

In sample SM, nagyágite lamellae show discontinuous, porous overgrowths consisting of yet another variety of nagyágite, different from the other two types (i.e., low-Pb) and skeletal hessite (Fig. 6a). Such overgrowths have a sharp, stepwise contact with the parent nagyágite, whereas their outer margin expands from the initial limit of the lamellae (Fig. 6b), thus differing from the symplectites in the two cases described above which more or less pseudomorph the lamellae. Hessite is pervasively distributed throughout the mass of low-Pb nagyágite. The larger hessite grain is 5–10 μm in size and is evenly interspersed by patches of even smaller size, lending the appearance of a mottled intergrowth between the two minerals. The composition of nagyágite in the overgrowths displays a comparable trend of As-enrichment to that of sample S2. In this case, however, the enrichment (up to 0.5 apfu As) is coupled with an increase in the Sb content (up to 1.5 apfu), rather than the decreasing trend as observed in sample S2. The net change is a decrease in the Pb content, by as much as 1 apfu. Patchy, larger masses of altaite and bournonite also occur in the overgrowths. They have an irregular distribution, appear to lack the porosity, and in some cases spread outside the overgrowth margin towards the parent nagyágite (Fig. 6b).

Sample SM also contains several areas with Ag-(Au)-tellurides that form a distinct Ag-rich assemblage, and in which nagyágite is present as only a minor, yet persistent component. The central mass of one such area is composed mainly of petzite (ca. 60%), within which Ag-rich domains are present. The latter consist of (i) hessite, stützite and petzite in equilibrium relationships (the phases meet at triple points; Fig. 6c), and (ii) hessite with fields of sylvanite exsolution (Fig. 6d). Other patches feature similar phase components as in Fig. 5c but petzite forms exsolutions in hessite in this case (Fig. 5e).

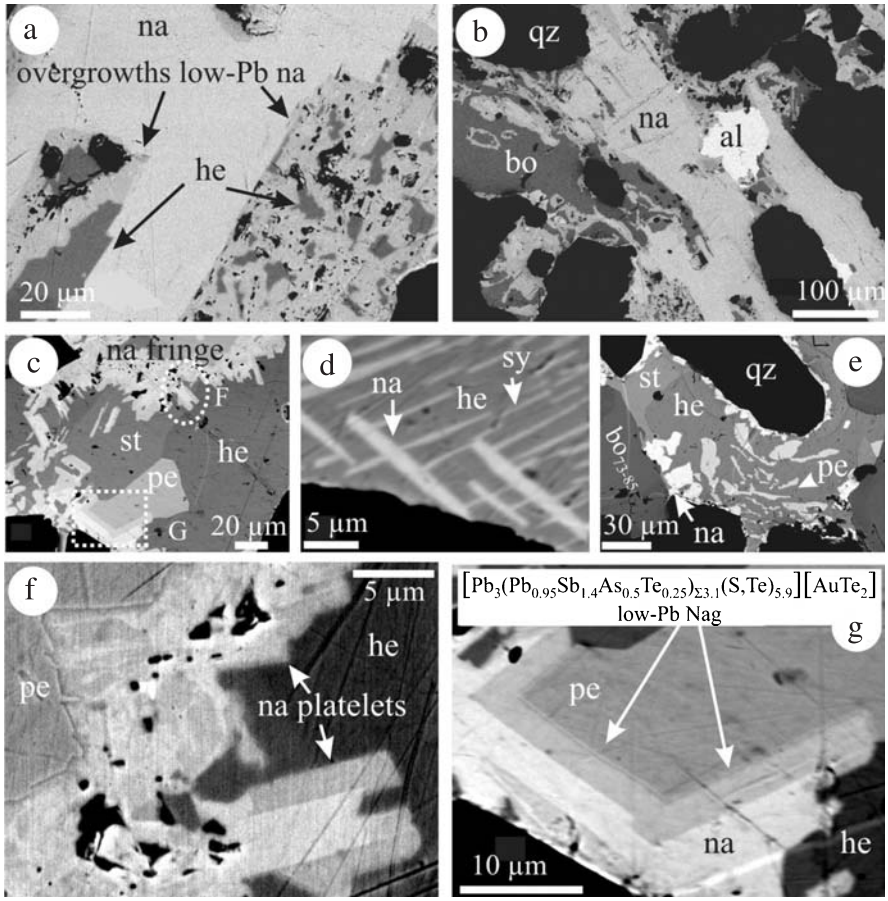

Fig. 6. BSE images of nagyágite in sample SM (Margareta vein). (**a**) Lamellae of 'normal' nagyágite (lighter) with overgrowth of low-Pb nagyágite (darker) and skeletal hessite; note the mottled texture in the overgrowths. (**b**) Larger masses of bournonite and altaite that have obliterated the contact between the overgrowth and parent nagyágite. (**c**–**g**) Nagyágite in a Ag-rich association. (**c**) Fringe of nagyágite platelets along boundaries between various Ag-(Au)tellurides. The latter meet at a triple point, indicating equilibrium conditions; note also the curvilinear boundaries between the phases at equilibrium indicating crystallization from a sub-solidus precipitate. (**d**) Two-stage exsolutions in hessite; nagyágite crosscuts former sylvanite. (**e**) Hessite with stützite along the margin and exsolutions of petzite; short platelets of nagyágite along the hessite margin. Note that this assemblage involves the same phases as in c, although different relationships feature here. (**f**) Typical zoned platelets of nagyágite. Low-Pb nagyágite outgrows resorbed cores of normal composition at the margin of the fringe, whereas chaotic zoning is seen in the smaller platelets along the same fringe. (**g**) Margin of petzite (detail from **c**) with nagyágite showing the same zoning as in **f**. Abbreviations are the same as in Figs. 3–5; *pe* Petzite; *st* stützite

Nagyágite is present as short platelets, strikingly different from the habit of the normal type, typically forming fringes placed along the mutual boundaries between the Ag-(Au)-tellurides (Fig. 6c). Nagyágite, exsolved after sylvanite (crosscutting relationships), is also observed exsolved from hessite (Fig. 6d). The platelets feature zonation with resorbed cores of normal nagyágite overgrown by margins of

low-Pb nagyágite; the latter is compositionally identical to the overgrowths described above. Simple zonation is characteristic for platelets at the outer margin aligned perpendicular to the direction of fringes (Fig. 5f), whereas a chaotic zonation is more typical of the smaller grains along the fringes. Exceptionally, zoned platelets occur singly or along the margin of one or the other host Au-Ag-tellurides (e.g., petzite, Fig. 5g).

Compositional data and plots

Microanalytical methodology

Electron probe microanalytical data were collected using a Cameca SX-51 instrument at Adelaide Microscopy Centre, University of Adelaide, Australia. Operating conditions were an accelerating voltage of 20 kV and a beam current of 20 nA. Standards used were: Au (Au), Bi_2Se_3 (Bi, Se), PbS (Pb, S), Ag_2Te (Ag, Te), Sb_2S_3 (Sb), CoAsS and GaAs (As).

Results

The compositions of nagyágite are shown in Table 2 and have been calculated on the basis of the 15-atom structural formula given by Effenberger et al. (1999); atoms per formula unit (apfu) hereafter always refers to such a 15-atom cell. This is considered most suited to express the chemical identity of nagyágite given the fact that the three-fold supercell is recognizable in electron diffraction images for normal nagyágite (Ciobanu et al., unpublished data). The data have been plotted in 7 binary diagrams and 1 ternary diagram (Figs. 7–9) that are discussed below. The positions of individual clusters are referred to ideal $[(Pb_3(Pb_2Sb)_{\Sigma 3})S_6][(AuTe_2)_3]$ composition and the regression lines are used to track the excess or deficiency for each respective variable relative to these ideal values; elemental substitutions resulting from these plots are given in Table 3. On all diagrams, except Fig. 8c and d, the analytical points form four clusters representing the following categories:

(i) Normal nagyágite, the largest cluster, typical for the long lamella in all three samples. Compositions from areas that appear darker on BSE images (Fig. 3c), as well as those from the tiles (Fig. 5d, e), are included and they separate into a distinct cluster (Au-depleted) on Fig. 8c and d. The normal cluster also comprises compositions from the middle part (cores) of platelets in sample SM (light on BSE images; Fig. 6f, g);
(ii) Low-Au nagyágite, lamellae nested in bournonite in sample S2 (Fig. 5f);
(iii) High-As nagyágite, the flaky lamellae in altaite in sample S2 (Fig. 5g), as well as a few points from the symplectites (Fig. 5c) and tiles (Fig. 5d, e) in the same sample;
(iv) Low-Pb nagyágite, the overgrowths (Fig. 6a) and margins of short-platelets in SM (dark on BSE images) (Fig. 6f, g).

For the purposes of this paper, we regard all of these as varieties of nagyágite, while acknowledging that crystal chemical data may subsequently confirm some of these to be distinct, but structurally closely related compounds.

Table 2. *Electron probe microanalyses of nagyágite (wt.%)*

	Ag	Au	Pb	Bi	As	Sb	Te	Se	S	Total
(A) 'Normal' nagyágite (Sample S3)										
Mean ($n = 31$)	0.07	10.52	56.25	0.22	0.26	7.80	15.16	0.13	10.64	101.06
S.D.	0.12	0.58	0.72	0.12	0.12	0.19	0.38	0.05	0.15	
Max.	0.58	11.36	57.34	0.42	0.65	8.17	16.03	0.21	10.95	
Min.	<mdl	9.50	55.06	<mdl	<mdl	7.35	14.33	<mdl	10.38	
Representative analyses										
S3.14.5	<mdl	10.09	55.90	0.31	0.28	7.69	15.06	0.05	10.79	100.17
S3.16.4	<mdl	9.57	56.55	0.09	0.32	7.77	15.78	0.12	10.91	101.11
S3 17.1	0.58	10.56	55.98	0.18	0.30	7.53	15.29	0.08	10.79	101.28
Atoms per formula unit (calculated to 15 atoms)										
Mean ($n = 31$)	0.01	0.95	4.82	0.02	0.06	1.14	2.11	0.03	5.89	
S3.14.5	–	0.91	4.79	0.03	0.07	1.12	2.10	0.01	5.98	
S3.16.4	0.02	0.85	4.79	0.01	0.06	1.12	2.15	0.03	5.97	
S3 17.1	0.09	0.94	4.75	0.02	0.07	1.09	2.11	0.02	5.91	
(B) 'Normal' nagyágite from platelets and overgrowths (Sample SM)										
Platelets										
Mean ($n = 6$)	0.12	10.12	55.43	<mdl	0.45	8.08	15.10	0.05	10.81	100.18
S.D.	0.10	0.21	0.67	–	0.31	0.54	0.36	0.04	0.20	
Max.	0.24	10.35	56.60	<mdl	1.05	8.53	15.48	0.10	11.12	
Min.	<mdl	9.76	54.68	<mdl	0.20	7.13	14.64	<mdl	10.56	
Representative analysis										
SM gr4 light	0.24	10.03	55.31	<mdl	0.32	8.24	14.64	0.03	11.12	99.92
Atoms per formula unit (calculated to 15 atoms)										
Mean ($n = 6$)	0.02	0.91	4.73	–	0.11	1.17	2.09	0.01	5.96	
SM gr4 light	0.04	0.89	4.69	–	0.07	1.19	2.02	0.01	6.09	
Overgrowths										
Mean ($n = 9$)	0.08	10.38	56.53	0.07	0.26	7.95	15.22	0.17	10.68	101.32
S.D.	0.09	0.24	0.51	0.10	0.06	0.25	0.28	0.09	0.13	
Max.	0.25	10.94	57.36	0.25	0.37	8.34	15.68	0.34	10.89	
Min.	–	10.17	55.54	–	0.17	7.57	14.76	0.07	10.52	
Representative analysis										
Sm2	<mdl	10.17	56.44	<mdl	0.17	7.74	14.76	0.13	10.64	100.04
Atoms per formula unit (calculated to 15 atoms)										
Mean ($n = 9$)	0.01	0.93	4.82	0.01	0.06	1.15	2.11	0.04	5.88	
Sm2	–	0.92	4.87	–	0.04	1.14	2.07	0.03	5.93	
(C) 'Au-depleted' nagyágite (Sample S3)										
Mean ($n = 19$)	0.07	7.72	56.84	0.28	0.23	7.92	16.92	0.10	10.81	100.88
S.D.	0.07	0.18	0.42	0.13	0.13	0.18	0.21	0.07	0.14	
Max.	0.20	8.19	57.56	0.67	0.40	8.32	17.29	0.24	11.02	
Min.	<mdl	7.45	56.00	0.08	<mdl	7.66	16.47	<mdl	10.54	

(*continued*)

Table 2 (*continued*)

	Ag	Au	Pb	Bi	As	Sb	Te	Se	S	Total
(C) 'Au-depleted' nagyágite (Sample S3)										
Representative analyses										
S3.19.4	<mdl	8.19	55.90	0.22	<mdl	7.79	16.47	<mdl	10.54	99.94
S3.14.1	<mdl	7.64	56.00	0.36	0.27	7.80	16.78	0.09	10.61	99.55
S3 15.5	0.16	7.46	56.92	0.26	0.28	7.73	16.49	0.16	10.94	100.41
Atoms per formula unit (calculated to 15 atoms)										
Mean ($n = 19$)	0.01	0.69	4.82	0.02	0.05	1.14	2.33	0.02	5.92	
S3.19.4	–	0.74	4.90	0.02	–	1.15	2.31	–	5.88	
S3.14.1	–	0.69	4.81	0.03	0.06	1.21	2.34	0.02	5.90	
S3 15.5	0.03	0.66	4.82	0.02	0.07	1.18	2.27	0.04	5.98	
(D) 'Au-depleted' nagyágite (Sample S2)										
Mean ($n = 7$)	0.05	7.59	56.84	0.20	0.49	7.73	17.11	0.06	10.99	101.06
S.D.	0.04	0.30	0.50	0.18	0.32	0.44	0.25	0.04	0.12	
Max.	0.09	7.89	57.57	0.47	1.11	8.16	17.52	0.12	11.16	
Min.	<mdl	6.99	56.18	<mdl	0.24	6.93	16.72	<mdl	10.85	
Representative analyses										
S2.11	0.07	6.99	56.52	0.12	0.77	7.97	16.72	0.12	11.09	100.38
S2.64	<mdl	7.79	56.96	0.06	0.35	7.41	17.07	<mdl	10.88	100.53
Atoms per formula unit (calculated to 15 atoms)										
Mean ($n = 7$)	0.01	0.67	4.77	0.02	0.11	1.10	2.33	0.01	5.97	
S2.11	0.01	0.62	4.74	0.01	0.18	1.14	2.28	0.03	6.01	
S2.64	–	0.69	4.83	–	0.08	1.07	2.35	–	5.96	
(E) Low-Au nagyágite (Sample S2)										
Mean ($n = 6$)	0.03	3.64	54.44	0.17	0.53	10.01	18.37	0.05	11.71	98.96
S.D.	0.05	0.14	0.27	0.14	0.07	0.13	0.15	0.04	0.07	
Max.	0.10	3.91	54.81	0.41	0.65	10.17	18.56	0.10	11.78	
Min.	<mdl	3.51	54.10	<mdl	0.45	9.78	18.17	<mdl	11.59	
Representative analyses										
S2p 36	<mdl	3.91	54.81	0.41	0.65	9.78	18.17	<mdl	11.68	99.40
S2p 40	<mdl	3.60	54.17	0.16	0.49	10.17	18.41	0.10	11.71	98.82
Atoms per formula unit (calculated to 15 atoms)										
Mean ($n = 6$)	–	0.31	4.47	0.01	0.12	1.40	2.45	0.01	6.21	
S2p 36	–	0.34	4.50	0.03	0.15	1.37	2.42	–	6.19	
S2p 40	–	0.31	4.45	0.01	0.11	1.42	2.46	0.02	6.22	
(F) High-As nagyágite (Sample S2)										
Mean ($n = 10$)	0.05	10.55	52.93	0.17	5.86	1.41	18.22	0.07	11.25	100.50
S.D.	0.05	0.40	0.99	0.12	0.44	0.76	0.35	0.05	0.12	
Max.	0.12	11.16	54.02	0.28	6.55	2.68	18.83	0.17	11.46	
Min.	<mdl	9.83	51.53	<mdl	5.14	0.26	17.64	<mdl	11.04	

(*continued*)

Table 2 (*continued*)

	Ag	Au	Pb	Bi	As	Sb	Te	Se	S	Total
(F) High-As nagyágite (Sample S2)										
Representative analyses										
S2p 24	0.06	10.45	51.53	<mdl	5.74	1.88	18.52	0.08	1.25	99.51
S2p 26	<mdl	10.61	52.82	0.25	6.07	1.10	18.18	0.03	11.46	100.38
S2p 61	<mdl	11.16	54.02	0.15	6.09	0.58	17.86	0.07	11.28	101.21
Atoms per formula unit (calculated to 15 atoms)										
Mean ($n = 10$)	0.01	0.90	4.28	0.01	1.31	0.19	2.39	0.02	5.88	
S2p 24	0.01	0.89	4.19	–	1.29	0.26	2.44	0.02	5.91	
S2p 26	–	0.90	4.25	0.02	1.35	0.14	2.38	–	5.96	
S2p 61	–	0.95	4.36	0.01	1.36	0.08	2.34	0.01	5.89	
(G) Low-Pb nagyágite from platelets and overgrowths (Sample SM)										
Platelets										
Mean ($n = 8$)	0.16	11.05	48.89	<mdl	2.13	9.96	18.29	0.10	10.76	101.35
S.D.	0.15	0.18	1.70	–	0.53	0.84	0.47	0.06	0.26	
Max.	0.44	11.24	51.62	<mdl	3.02	10.88	18.61	0.16	11.03	
Min.	<mdl	10.66	46.18	<mdl	1.49	8.66	17.19	<mdl	10.38	
Representative analysis										
SM gr4 dark	0.05	11.00	48.39	<mdl	3.02	9.26	18.31	0.08	10.93	101.05
SM gr7 dark	0.27	10.66	47.25	<mdl	2.54	10.56	18.60	0.16	10.43	100.47
Atoms per formula unit (calculated to 15 atoms)										
Mean ($n = 8$)	0.03	0.95	4.00	–	0.48	1.39	2.43	0.02	5.70	
SM gr4 dark	0.01	0.93	3.93	–	0.68	1.28	2.41	0.02	5.73	
SM gr7 dark	0.04	0.89	3.89	–	0.58	1.48	2.49	0.04	5.55	
Overgrowths										
Mean ($n = 4$)	0.13	11.21	47.83	<mdl	2.08	10.93	18.98	<mdl	11.08	102.23
S.D.	0.20	0.12	0.86	–	0.24	0.28	0.47	–	0.08	
Max.	0.43	11.38	49.00	<mdl	2.35	11.30	19.24	<mdl	11.16	
Min.	<mdl	11.11	46.97	<mdl	1.79	10.65	18.28	<mdl	10.96	
Representative analysis										
Sm1 72	<mdl	11.12	49.00	<mdl	1.79	10.65	18.28	<mdl	11.16	101.99
Atoms per formula unit (calculated to 15 atoms)										
Mean ($n = 4$)	0.02	0.95	3.84	–	0.46	1.49	2.47	0.01	5.75	
Sm1 72	–	0.95	3.96	–	0.40	1.47	2.40	–	5.83	

<*mdl* less than minimum detection limit (0.02–0.03 wt.%)

General sums of atoms in the two types of layers

On the plots in Fig. 7, only the normal nagyágite is close to ideal, with minor Au + Te excess and S deficit (< 0.1 apfu for the cluster center). This cluster, as well as those with low-Au, are centered onto the Pb + Sb + As = 6 position, where-

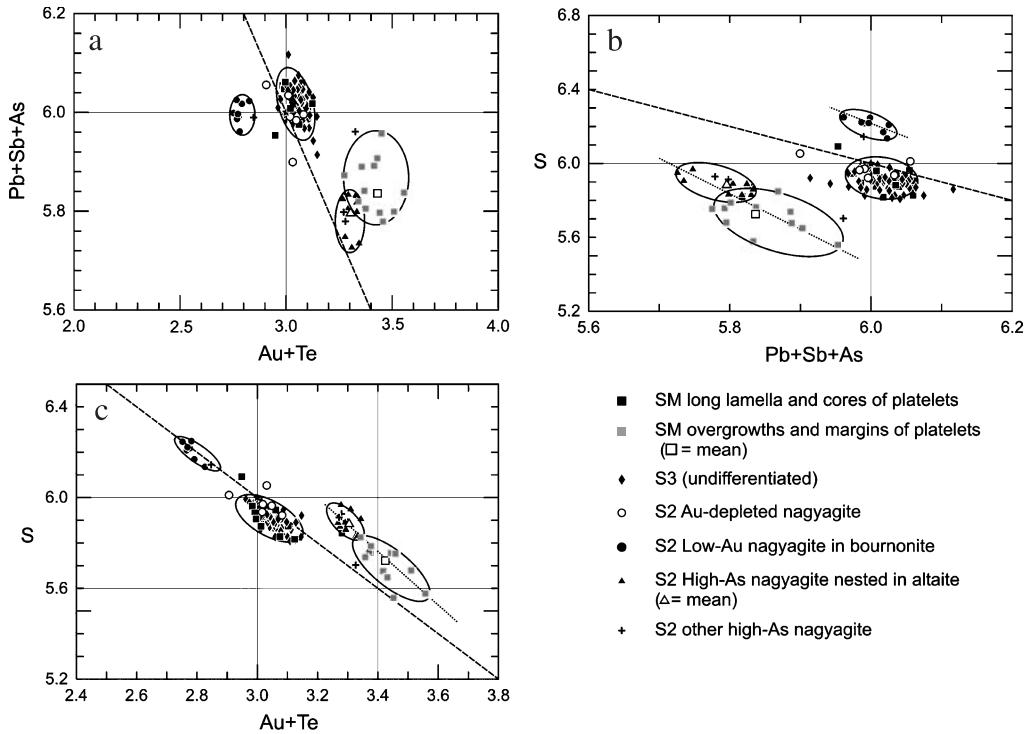

Fig. 7. Binary diagrams illustrating compositional variation in nagyágite in terms of the total sums of atoms (per formula unit) in the two types of layers, calculating formulae to a total of 15 atoms: (**a**) (Pb + Sb + As) *vs.* (Au + Te). (**b**) S *vs.* (Pb + Sb + As). (**c**) S *vs.* (Au + Te). See accompanying text for explanation and discussion

as the other two clusters (high-As and low-Pb) show a marked deficit from this value (Fig. 7a, b). The latter two also display Au + Te excess and S deficit; the low-Au variety shows the inverse trends between the same variables. Opposing trends between Au + Te and S are indicative of substitutions between these elements that are otherwise concentrated in the different layers. This becomes clear from Fig. 7c that shows all clusters drawn along (low-Au, normal) or above (high-As, low-Pb) the regression line. The offset observed for the high-As and low-Pb clusters, corroborated with their deficits in the Pb + Sb + As sum (Fig. 7a), indicates that, in these varieties, both cations and S in the Q modules have deficits that are compensated by an excess of one or the other element forming the telluride layer (i.e., Te values that are higher than the ideal 2 apfu in all cases, Table 2).

The Me_2 site in the sulfosalt layer

Substitution Sb(+ As) → Pb in the Me_2 site is plotted in Fig. 8a. The low-Au and high-As form clusters mid-way, and at comparable values (Pb-3 = 1.5 and 1.3 apfu, respectively) between the normal (Pb-3 = 1.8 apfu; close to ideal) and low-Pb (Pb-3 = 1 apfu) clusters. The values are given for means of the clusters in Table 3. The high-As and low-Pb clusters fall along a regression line below that of the ideal composition (Fig. 8a), because they have deficits in the Me_2 site.

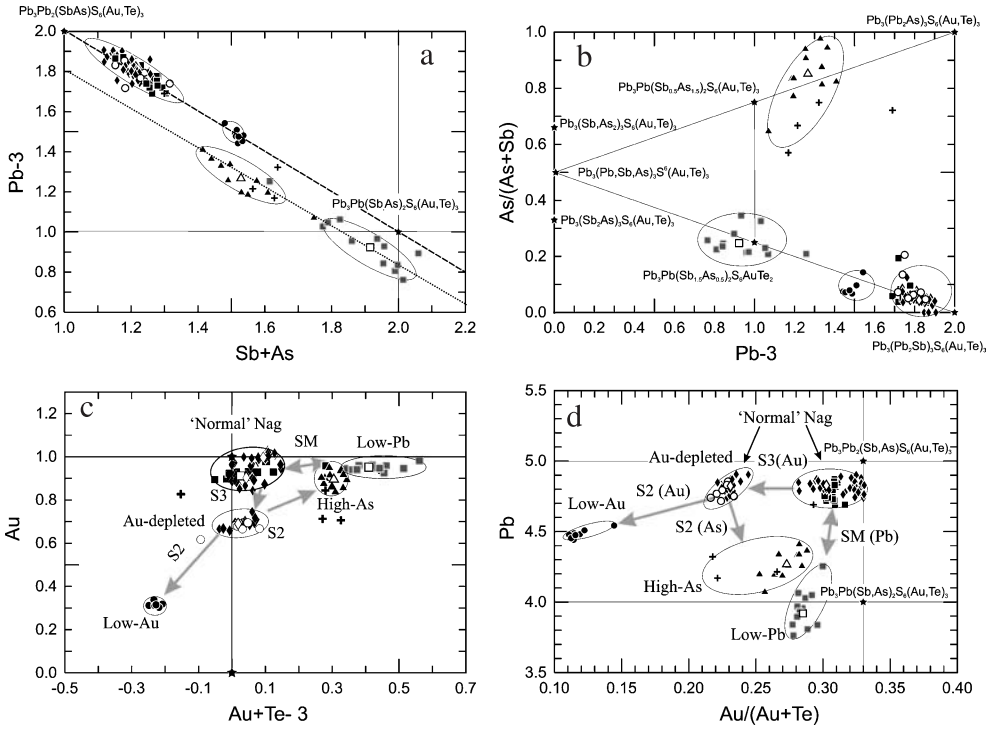

Fig. 8. Set of binary diagrams illustrating compositional variation in nagyágite in terms of variation in atoms in the Me_2 site (per formula unit), calculating formulae to a total of 15 atoms. (**a**) Pb-3 *vs.* (Sb + As). (**b**) As/(As + Sb) *vs.* Pb-3; and in (**c**) in terms of Au trends relative to occupancy in the telluride layer, Au *vs.* (Au + Te-3) and (in **d**) in both layers, Pb *vs.* Au/(Au + Te). See accompanying text for explanation and discussion. Symbols used are the same as in Fig. 7

The dataset shows variable As-enrichment trends, expressed as As/(As + Sb) (Fig. 8b). The clusters relate to two different tie lines that link Pb-free, intermediate As/Sb nagyágite (Pb-3 = 0, As/(As + Sb) = 0.5) on one side, with an ideal high-Pb (Pb-3 = 2 apfu) that is either (i) the pure Sb end-member, or (ii) the pure As end-member on the other. The normal, low-Au and low-Pb clusters are placed along the same regression line (i). The low-Pb composition (Pb-3 = 1 apfu) occurs at As/(As + Sb) = 0.25 apfu (Table 3). In this case, Pb variation is tightly coupled to substitution by Sb + As. The high-As cluster straddles the other regression line (ii), with the mean at As/(As + Sb) = 0.8 and Pb-3 = 1.3 apfu. However, the scatter of points shows an inverse correlation, with regression line (ii) indicating that a second substitution As → Sb, with opposite trend to Sb + As → Pb, is responsible for Me_2 variation in the high-As cluster.

Gold variation

Variation in Au, as shown by (Au + Te)-3 or the Au/Au + Te ratio, shows discrete compositional clusters that are not linked by any continuous trend (Fig. 8c, d). The Au-depleted population splits from the normal nagyágite cluster, with a distinct Au

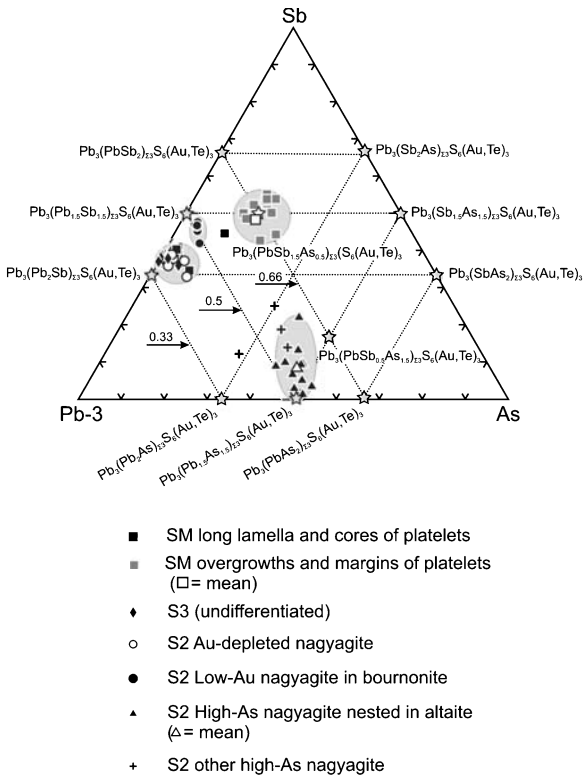

Fig. 9. Compositional variation in nagyágite shown in a ternary diagram showing occupancy in the Me_2 site, (Pb-3)-Sb-As. Lines labeled as '0.33', '0.5' and '0.66' indicate $(Sb + As)/(Pb\text{-}3 + Sb + As)$ ratios. Filled star indicates the composition of ideal nagyágite. The diagram does not show the Te substituting in Me_2

content and $Au/(Au + Te)$ ratio, which also differs from those in the low-Au cluster. The 'low-Au' variety forms a tight cluster at lower Pb and with an apparent deficit in the telluride layer (see above). Thus the 'Au-depleted' variety is derived from the normal nagyágite by the simple substitution of Te for Au at around 0.31 apfu, leading to a content of $Au = 0.69$ apfu, at constant Pb. In this case, the $Au/(Au + Te)$ ratio represents a true measure of Au decrease from one cluster to another (i.e., from 0.31 to 0.23 apfu). In the low-Pb and high-As clusters, the Te excess (as discussed above) is seen in Fig. 8c in the positive balance of atoms in the telluride layer at close to ideal Au values is responsible for the apparent lower $Au/(Au + Te)$ ratios (0.28 and 0.27, respectively). The spreads in these clusters show positive correlation trends between Pb and $Au/(Au + Te)$ ratios (Fig. 8d), in turn indicating an inverse correlation between Pb and Te.

The main varieties of nagyágite at Săcărîmb

The ternary diagram in Fig. 9 delineates the main compositional varieties of nagyágite at Săcărîmb as defined by the variation of metals in the Me_2 site. This can be expressed as tie lines with $(Sb + As)/(Pb\text{-}3 + Sb + As)$ varying from 0.33 ($Sb + As = 1$ apfu) to 0.66 ($Sb + As = 2$ apfu). Normal nagyágite (including the points representing Au-depleted nagyágite) forms a tight cluster lying between the tie lines 0.33 and 0.5, at ca. 0.4, close to ideal nagyágite, although with a slight As-shift. The low-Au nagyágite falls on the 0.5 tie line, but is also

Table 3. *Compositional data with sums and interpreted substitutions in different types of nagyágite and in the literature referred to in the text*

	'Normal'	Au-depleted		Low-Au			High-As		Low-Pb	
Wt.%	A + B ($n = 46$)	C + D ($n = 26$)	Effenberger et al. (1999) synth ($n = 18$)	E ($n = 6$)	Cioflica et al. (1993a, b) ($n = 1$)	Lupulescu, 1997 ($n = 1$)	F ($n = 10$)	Simon et al. (1994) $n = 53$	G ($n = 12$)	Effenberger et al. (1999) synth
Bi	0.16	0.26	–	0.17	–	–	0.17	–	–	–
Pb	56.20	56.84	55.79	54.44	57.22	56.66	52.93	53.10	48.54	45.99
Au	10.44	7.69	7.83	3.64	3.62	3.43	10.55	10.10	11.10	7.83
Ag	0.08	0.07	–	0.03	0.03	0.04	0.05	0.10	0.16	–
Sb	7.87	7.87	8.7	10.01	9.87	9.88	1.41	3.20	10.28	11.42
As	0.29	0.30	–	0.53	–	–	5.86	4.00	2.12	–
Te	15.16	16.97	18.36	18.37	18.22	17.99	18.22	18.10	18.52	24.35
Se	0.13	0.09	–	0.05	–	–	0.08	–	0.09	–
S	10.67	10.86	11.02	11.71	12.08	11.99	11.25	11.20	10.87	10.27
Total	101.1	100.9	101.7	99.0	101.0	100.0	100.5	99.8	101.7	99.9
Recalculated formula unit (on basis of 15 atoms; see also accompanying text)										
Pb(+Bi) (total)	4.81	4.82	4.65	4.48	4.63	4.62	4.29	4.37	3.95	3.84
Sb (Me_2)	1.14	1.13	1.23	1.40	1.36	1.37	0.19	0.45	1.42	1.62
As (Me_2)	0.07	0.07	–	0.12	–	–	1.31	0.91	0.48	–
Au (+Ag)	0.95	0.69	0.69	0.32	0.31	0.30	0.91	0.89	0.97	0.69
Te (total)	2..10	2.33	2.49	2.45	2.39	2.38	2.39	2.42	2.45	3.30
S (+Se)	*5.92*	*5.95*	*5.94*	*5.99*	*6.00*	*6.00*	*5.90*	*5.96*	*5.73*	*5.54*
Pb + Sb + As	*6.03*	*6.03*	*5.89*	*6.00*	*5.98*	*5.99*	*5.80*	*5.73*	*5.85*	*5.47*
Pb-3 (Me_2) $(2 - x)$	1.80	1.80	1.65	1.47	1.63	1.62	1.28	1.37	0.95	0.84
Sb + As (in Me_2)	1.21	1.20	1.23	1.52	1.36	1.37	1.506	1.36	1.90	1.62
Au + Te	*3.06*	*3.02*	*3.17*	*2.77*	*2.70*	*2.68*	*3.30*	*3.29*	*3.42*	*3.99*

(*continued*)

Table 3 (*continued*)

Wt.%	'normal' A + B ($n = 46$)	Au-depleted C + D ($n = 26$)	Au-depleted Effenberger et al. (1999) synth ($n = 18$)	Low-Au E ($n = 6$)	Low-Au Cioflica et al. (1993a, b) ($n = 1$)	Low-Au Lupulescu, 1997 ($n = 1$)	High-As F ($n = 10$)	High-As Simon et al. (1994) $n = 53$	Low-Pb G ($n = 12$)	Low-Pb Effenberger et al. (1999) synth
Interpreted substitutions (see also footnote)										
(Sb + As)-1 = a	0.20	0.20	0.23	0.52	0.36	0.38	0.505	0.36	0.90	0.62
Te (Me_2) = b	–	–	0.13	–	–	–	0.24	0.29	0.25	0.72
($a + b$) = x	0.20	0.20	0.36	0.52	0.36	0.38	0.76	0.65	1.15	1.34
Te (S site) = y	0.04	0.02	0.04	–	–	–	0.06	0.02	0.17	0.27
Te for Au (X) = z	0.05	0.31	0.31	0.45	0.39	0.38	0.09	0.11	0.03	0.31
S for (Au,Te) (X) = w	–	–	–	0.23	0.31	0.32	–	–	–	–
Recalculated sums with substitutional values										
Pb + Sb + As + Te_b	6.03	6.03	6.02	6.00	5.98	5.99	6.04	6.02	6.10	6.19
(S-S_w) + Se + Te_y	5.96	5.97	5.98	5.99	6.00	6.00	5.96	5.98	5.90	5.81
(Au + (2 + Te_z) + S_w) (T)	3.00	2.99	3.00	2.99	3.01	2.99	2.99	2.98	2.98	3.00
Bond valence for Q modules										
Me_1 (3Pb)	4.63	4.63	4.63	4.63	4.63	4.63	4.63	4.63	4.63	4.63
Me_2	6.78	6.76	6.75	6.50	6.67	6.69	5.55	5.89	6.12	6.59
Sum cations	11.41	11.39	11.38	11.13	11.30	11.32	10.18	10.52	10.75	11.22
Anions	11.43	11.38	11.41	11.13	11.34	11.33	10.19	10.49	10.82	11.19

General formula: $(Pb_3S_3)[(Pb_{2-x})(Sb,As,Te_b)_{1+x}(S_{3-y}Te_y)]_{\Sigma 6}(Au_{1-z-w}Te_{2+z}S_w)$, where $b = x + 1 - (Sb + As)$; $0.2 < x < 1.15$; $0 < b < 0.29$. Empirical values of y, z and w: $0 < y < 0.17$; $0 < z < 0.45$; $0 < w < 0.32$

Charge $Me_1 = 3Pb \times 1.543$; Charge $Me_2 = (Pb\text{-}3 \times 2.506) + ((Sb + Te_b) \times 1.913) + (As \times 1.145)$; Charge anions = inverse charges of (S-Sw) + Se + Te_y to metals (3Pb + x) as in cation charge balance, and with modified bond valencies in cases where Te_y is also involved

slightly shifted towards As. The low-Pb nagyágite is centered on the composition $Pb_3Pb(Sb_{1.5},As_{0.5})_{\Sigma 2}S_6(Au,Te)_3$, along the tie line at a (Sb + As)/(Pb-3 + Sb + As) value of 0.66. The high-As cluster reaches the As-end of the tie line at 0.5, with a spread towards the tie line at 0.66. Even though some of the points are close to the As-end member, $Pb_3(Pb_{1.5},As_{1.5})_{\Sigma 3}S_6(Au,Te)_3$, the mean is shifted towards $Pb_3Pb(As_{1.5},Sb_{0.5})_{\Sigma 2}S_6$ $(Au,Te)_3$.

Discussion

Nagyágite characterization

The compositional variation in type locality nagyágite documented above and in previous publications, draws attention to several types of substitutions not indicated by the general formula of Effenberger et al. (1999). Secondly, there are three varieties that significantly differ from the composition of 'ideal' nagyágite; all display higher degrees of substitution by Me^{3+} for Pb in the mixed site of the sulfosalt layer. They could thus represent targets for investigation of metal ordering in this site, which is one way to obtain derivatives from a parent structure. High-As nagyágite is distinct from ideal nagyágite (As-free) as currently considered, and this may qualify as a new mineral requiring a full crystal-structure characterization.

In Table 3, the compositional data for distinct varieties of nagyágite have been summarized, along with key data from the literature (Cioflica et al., 1993a, b; Simon et al., 1994; Lupulescu, 1997; Effenberger et al., 1999). We have performed a series of calculations to derive a general formula for nagyágite that incorporates several inferred substitutions. We first consider the sulfosalt (Q) modules, assuming full occupancy of the Me_1 site by Pb (3 apfu). We also assume close to full occupancy of the Me_2 site (3 apfu) by Pb (Pb_{total}-3), Sb and As, with the sum of atoms in the Q modules equal to 12 (Me_2 + associated S is 6).

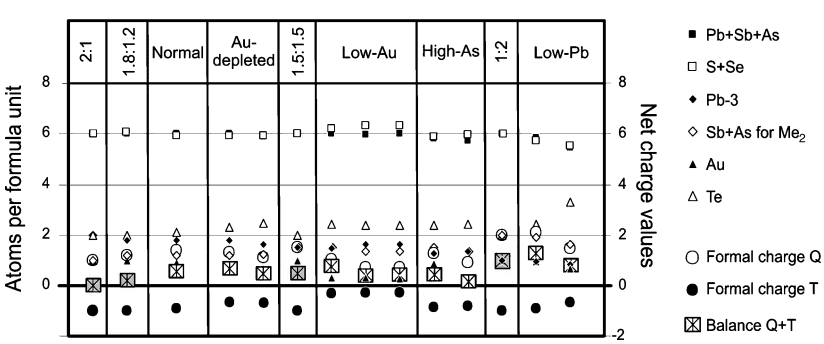

Fig. 10. Diagram illustrating the compositional varieties of nagyágite discussed in terms of atoms per formula unit of the principal components. The diagram corresponds to the columns in Table 3, left to right. 2:1, 1.8:1.2, 1.5:1.5 and 1:2 correspond to ideal compositions where these numbers correspond to the ratio between Pb and Me^{3+} in the Me2 site. Formal charge balance in the Q module and T layer and the net difference between the two are also shown. The charge for T takes Te (as Te^{2-}) only for that Te bound to gold in the ratio 1:2. Remaining Te (and S) in the layer is considered as formally zerovalent

Substitution of atoms in the Me_2 site in terms of nominal formal valencies (Pb^{2+}, Sb^{3+}, As^{3+}, S^{2-} etc.) that may appear to constrain oxidation states of atoms in the sulfosalt layers relative to atoms in the T layer (Te^{2-} and Au^{3+}), do not, however, give consistent charge balances (or electroneutrality) throughout the dataset (Fig. 10). Even in nagyágite with composition $(Pb_3(Pb_{1.8}Sb_{1.2})_{\Sigma 3}S_3)AuTe_2$, the sulfosalt layer has a net positive charge of +1.2, and that of the T layer has a −1.0 net negative change, giving a slight mismatch of +0.2. In all cases, the formal charge balance in the T layer is made by considering only the amount of Te bound to Au, keeping a ratio of 1:2. This is because accommodation of Te in excess of that bound to gold (2:1), as additional Te rows between the Au arrays in the T layer via stacking errors, would necessitate a formally zerovalent status for this Te. Net formal charge balance for ideal compositions (Fig. 10) shows that increased Me^{3+} substitution offsets this value from zero (2Pb:1Me^{3+}) to +1 (1Pb:2Me^{3+}). The formal charge balance between the layers thus appears strong in ideal nagyágites, indicating 'ionic' bonds between the two units. Such a view is not validated by

Table 4. *Atomic distances [in Å, from Effenberger et al. (1999)] and bond valences [calculated after Brese and O'Keeffe (1991)] for the sulfosalt layer in nagyágite*

Atom 1	Atom 2	Atomic distance	Bond valence			
Me_1 (Pb)	S2	2.885		0.405		
	S1[a] (2×)	3.011		0.287		
	S1[b] (2×)	3.018		0.282		
				Total (5 bonds) 1.543		
			$Me_2 = Pb$	$Me_2 = Sb$ (Te)		$Me_2 = As$
Me_2	S1	2.562	0.969	0.740		0.443
	S2[a] (2×)	2.767	0.556	0.424		0.254
	S2[b] (2×)	3.198	0.173	0.132		0.079
	S2[c]	3.488	0.079	0.061		0.036
			Σ (6) 2.506	Σ (6) 1.913		Σ (6) 1.145
Me_1 (Pb)	Te	3.619		0.122		
	Te (2x)	3.641		0.115		
	Te	3.656		0.110		
				Total (5 bonds) 0.462		
			$Me_2 = Pb$	$Me_2 = Sb$	$Me_2 = As$	$Me_2 = Te$
Me_2	Te1	2.562	2.123	1.805	1.140	1.701
	Te2[a] (2×)	2.767	1.217	1.035	0.654	0.980
	Te2[b] (2×)	3.198	0.380	0.323	0.204	0.306
	Te2[c]	3.488	0.174	0.148	0.093	0.140
			Σ (6) 5.489	Σ (6) 4.668	Σ (6) 2.948	Σ (6) 4.335

Bond valence parameters (Brese and O'Keeffe, 1991)
Pb-S 2.55, Pb-Te 2.84, Sb-S 2.45, As-S 2.26, Bi-S 2.55, Te-S 2.45, Sb-Te 2.78, As-Te 2.61, Te-Te 2.76
Equation: $v_{ij} = \exp[(R_{ij} - d_{ij})/b]$, where v_{ij} is the bond valence between two atoms 1 and j, d_{ij} is the bond distance between the two atoms, R_{ij} is the bond valence parameter and b is a universal constant (0.37å)

what is known about the structure (Effenberger et al., 1999, 2000). Instead, in nagyágite, the presence of monovalent Au atoms that may be accommodated by local displacements or of varying ratios of covalent Te-Te bonds and unbonded Te-Te contacts may adjust formal charge balance (Effenberger et al., 1999).

We have chosen to calculate the charge balance in the Q modules using the bond valence method of Brese and O'Keeffe (1991). This procedure allows us to take cation-anion bond valence parameters into consideration, and evaluate the total bond valence for individual atoms in site Me_2 (Table 4). Such an approach has been undertaken, for example, by Lafond et al. (1997) to address the covalent character of layered composite incommensurate compounds with comparable SnS modules. The method allows us to check charge neutrality between metals and sulfur within the sulfosalt layer. The usefulness and applicability of combining the bond length data given in Effenberger et al. (1999) with substitutions that were not recognized in that work, as well as the problematic nature of calculating formal bond valances for such partly covalent compounds, may be considered questionable. Accepting the limitations of our approach, in particular the relative importance of covalent bonding at the expense of formal charge valencies for some substitutions such as Te within Me_2, we nevertheless believe it to be appropriate as a first attempt to better appreciate likely substitution mechanisms.

In Table 3, term '*a*' represents (Sb + As)-1 in the Me_2 site. In the case of As-rich and low-Pb nagyágite, a remaining deficiency in the Me_2 site relative to sulfur can be met by an additional substitution, by Te ('*b*'), since that element is in apparent excess to the total atoms in the T layer. The term '*x*' represents the sum of *a* and *b*, the sum of atoms substituted within Me_2 relative to $(Pb_3(Pb_2Sb_1)_{\Sigma 3}S_6)AuTe_2$. Recalculation of published data for the high-As variety (Şimon et al., 1994; average of 53 points) gives a similar result (i.e., the Me_2 deficit is compensated by Te excess at 0.29 apfu, Table 3).

The Te-rich character of some varieties of nagyágite from Săcărîmb has been noted by Lupulescu (1997) and Shimizu and Stanley (2003), among others. In the present dataset, it is only the normal nagyágite that has the ideal amount of Te (2 apfu) (Tables 2 and 3). In the Au-depleted and low-Au varieties (and also in the published data of Cioflica et al., 1993 and Lupulescu, 1997 for low-Au), the excess Te compensates for the Au deficit in the T layer (term '*z*'). In these cases, there is no deficiency in the Me_2 site to be met by Te. Excess Te also compensate for the modest Au deficiencies in As-rich and low-Pb nagyágite.

In the low-Au variety, compensation of the Au deficit by excess Te still reveals an overall deficiency in the T layer, indicating a further substitution. Given the configuration of the T layer (Effenberger et al., 1999), we suggest that S substitutes for Te (term '*w*'), presumably *via* isovalent exchange $S^{2-} \rightarrow Te^{2-}$. Availability of excess S, beyond the amount necessary for charge balance in the Q modules, is indicated by the calculations above.

In the Au-depleted, As-rich and low-Pb nagyágite, there is no S-excess, but rather a deficiency, as indicated by bond valence considerations. In these three cases, as well as to a limited extent even in normal nagyágite, there is still an excess of Te, after compensation for Au bringing the total of atoms in the T layer to 3, and after compensation of any deficiency in the Me_2 layer. We thus assign the remaining Te excess to S in the Q modules (term '*y*'). Minor substitution of Te^{2-}

for S^{2-}, at values comparable to those indicated here, is common in a wide range of sulfosalts.

The weakness of any bonds across the sulfosalt and T layers is indicated by the bond valence method applied to Me_1 (Pb). This shows that the strength of the bond to S in the Q is three times higher than the corresponding bond valence for Me_1 (Pb) to Te in the T layer (Table 4).

The synthetic product obtained by Effenberger et al. (1999), which can be considered an analogue of the low-Pb nagyágite, shows the highest Te excess. Using this procedure, this might be explained in terms of compensation for Au (0.31 apfu), Me_2 (0.72 apfu) and S (0.27 apfu) (Table 3).

Consideration of the available information (Table 3) allows us to propose the following general formula for nagyágite: $Pb_3S_3[(Pb_{2-x})(Sb,As,Te_b)_{1+x}]_{\Sigma 3}(S_{3-y}Te_y)_3(Au_{1-z-w}Te_{2+z}S_w)$, where $b = x + 1 - (Sb + As)$; $b = 0$ to 0.29; $0.2 < x < 1.15$. Empirical values of y, z and w: $0 < y < 0.17$; $0 < z < 0.45$; $0 < w < 0.32$. The aforementioned synthetic low-Pb product shows higher values of b, x and y.

Why are there so many varieties of 'nagyágite' at Săcărîmb?

Replacement via coupled dissolution-(re)precipitation reactions

The breakdown and wide range of chemical variation in nagyágite from Săcărîmb is mostly tied to pseudomorphism, a key feature in mineral replacement by coupled dissolution-(re)precipitation reactions (e.g., Putnis, 2002). Preservation of crystal shape is possible if the rate of product precipitation is equilibrated stepwise by the rate of dissolution of the parent mineral. The advance of the replacement front is dependent upon many factors, among which generation of porosity and solubility of parent crystal in the fluid are both of prime relevance here. Both impact upon the local supersaturation of the dissolved phase in the pervading fluid. Tenailleau et al. (2006) reported the first experimental studies of coupled dissolution-reprecipitation reactions in sulfide minerals in the pentlandite-violarite system.

Replacement with molar-excess reaction

Replacement textures may indicate if the reaction is with molar deficit or excess. The latter can be associated with formation of symplectites if the fluid becomes saturated with respect to two new phases during replacement (Putnis, 2006), as seen in the breakdown of nagyágite to galena-altaite symplectites (Fig. 3a–c). The indicative feature for molar excess is the irregular advance of replacement (Putnis, 2002), which in this case forms deep inliers controlled by cleavage. Gold depletion in nagyágite adjacent to decomposition indicates that diffusion played a role, simultaneous with infiltration that assists breakdown.

Porosity may be a transient phenomenon when obliterated by textural re-equilibration (Putnis, 2002), such as the pseudomorphosis of nagyágite by galena (Fig. 4a). This is observed in the same sample where nagyágite features symplectites that retain porosity (Fig. 3d). Such aspects, seen in areas no more than a few mm apart, and involving replacement of the same mineral in a common matrix, suggest that other factors such as infiltration rates were variable in the pervading

fluid. A slower infiltration rate would obliterate the breakdown and lead to complete replacement by galena; Au resulting from this reaction will precipitate in the surrounding carbonate halo (Fig. 4).

Replacement with molar-deficit reaction

An intermediate stage of reaction is retained in the areas of decomposition with 'tiled' appearance (Fig. 5d, e), between altaite and bournonite, and which host high-As and low-Au nagyágite, respectively (Fig. 5c, f–g). This interpretation is based upon the fact that the same elemental trends, [i.e., Au-depletion *via* Te for Au substitution and As-enrichment *via* As for Sb + Pb substitution, observed together, from one tile to the next (each only a few microns across)] are also present alone in separate areas. The apparent inverse trends between Au and As (also observed in the symplectitic halos; Fig. 5b), suggest that they are coupled to adjust variable reaction rates between the same parent nagyágite and the pervading fluid. Preservation of such trends at variable degrees of substitution indicates, however, that replacement is controlled by local chemical gradients at a scale more likely to indicate diffusion than an infiltration-driven fluid.

Maximum values of the two exchange reactions above are attained in areas from the same lamella where the infiltration threshold is enhanced, leading to reprecipitation of low-Au and As-rich nagyágite. The two varieties share comparable degrees of substitution of Pb by Sb + As in the Me_2 site (Fig. 9), a substitution barely present in the Au-depleted variety. This implies that other elements (e.g., Pb), become mobile only during infiltration-driven replacement. Gold, on the other hand, may be easily remobilized by diffusion if Te is available to replace it.

In terms of amount of Au *vs*. telluride layer occupancy, the two highly substituted varieties of nagyágite form the ends of a line encompassing the Au-depleted variety at zero excess/deficit (Fig. 8c). The latter is, however, not affected by changes in the amount of Pb, as in the others (Fig. 8d). We thus consider the Au-depleted variety as a relict resulting from parent nagyágite by diffusion-assisted remobilization of Au. This accounts for nucleation of sylvanite, which is always observed in conjunction with the tiled areas (with volume increase; Fig. 5e), if the fluid provides Ag. In contrast, the low-Au and As-rich nagyágite represent (re)precipitation products of infiltration-driven replacement of the same parent nagyágite. Based on these aspects, and despite the fact that the infiltration rates may vary across the same lamella, we suggest that replacement is with molar deficit in this case, forming two of the three highly substituted varieties of nagyágite.

The sharp and stepwise contact of the overgrowths containing the low-Pb nagyágite towards the parent lamella is indicative of a molar deficit reaction. This is the case when the front moves through the crystal interface leaving behind a mass of porous precipitate (Putnis, 2002). This is also underlined by the rapid growth of components in the precipitate (i.e., skeletal hessite, mottled texture with low-Pb nagyágite). In contrast, other minerals tied to the same overgrowths (e.g., altaite, bournonite) seem to have formed at the expense of the overgrowths themselves, rather than contemporaneously with the advance of dissolution front, since they obliterate – in places – the initial contact between the overgrowths and parent lamella (Fig. 6b).

Residual nagyágite formed from Ag-rich precipitates

A compositional replica of the nagyágite varieties above is seen in the zoned platelets forming fringes in and around crystal boundaries of Ag-(Au)-tellurides (Fig. 6c). The crystal zonation, low-Pb nagyágite outgrowing resorbed cores of normal nagyágite, features a trend that indicates a cycle of Pb-depletion and Sb + As saturation following nucleation of 'normal' nagyágite. This trend may be recurrent in the clustered, smaller platelets along the fringes that show chaotic oscillatory zonation (Fig. 6f). Such differences in the zonation patterns can be explained in terms of more rapid nucleation, denser population of crystallizing nuclei, of nagyágite in the inner part of the fringe relative to the margin.

The nagyágite platelets, which crystallized after the host Ag-(Au)-tellurides, can be considered to result from a residual mash, interstitial to grain boundaries, which gradually incorporated those elements exotic to the main Ag-Au-Te phases that underwent crystallization upon cooling. The Ag-Au-Te phases encountered phase separation at equilibrium following precipitation (e.g., curvilinear boundaries between phases, as in Fig. 6c). This may be considered the equivalent of $\beta Ag_{5\text{-}3}Te_3$-$\beta Ag_2Te$-$Ag_3AuTe_2$, an assemblage that, even though could not be obtained experimentally, was nonetheless discussed by Cabri (1965) to result upon heating at 315 °C from one of the two alloys prepared by Markham (1960) with composition lying in the $AgAuTe_4$-Ag_3AuTe_2-Ag_2Te phase region of the Au-Ag-Te system at 300 °C. Exsolutions among Au-Ag-tellurides (Fig. 6d, e) represent the low temperature products of the 'χ' phase of Cabri (1965). 'χ' phase is considered stable from 1.5 to 9 at.% Au, in the temperature range 415–450 °C, and along the tie line Ag_2Te-Ag_3AuTe_2 at 33.33 at.% in the system Au-Ag-Te. Even though all observed assemblages can be tied to this section in the system Au-Ag-Te, each patch may have a slightly different composition upon precipitation, accounting for the variation in the associations from one patch to another. Evidence that nagyágite and the host tellurides are part of the same precipitate is seen in the nagyágite exsolved from hessite (Fig. 6d) or that formed at the grain boundaries of petzite (Fig. 6g).

Zonation in nagyágite can be associated with self-patterning phenomena occurring due to small chemical fluctuations in closed systems (e.g., Ortoleva, 1994). The residual mash interstitial to the Au-Ag-tellurides may be considered as one such system. Depletion of Pb and saturation of Sb + As in the mash is induced by crystallization of normal nagyágite cores and this provides the oscillatory trigger for the observed zonation. The extent of As + Sb for Pb substitution is similar to that recorded during replacement of nagyágite by the overgrowths, suggesting a common source for the causative fluids.

Petrogenetic implications

The prerequisite of mineral replacement, which may be fluid-driven in hydrothermal systems, is disequilibrium between the pervading fluid and a parent mineral (e.g., Putnis, 2002), in this case nagyágite, which in all samples shows a dominant normal, close to ideal composition. Secondly, in coupled dissolution-reprecipitation reactions, although the advance of the replacement front is dependent upon

maintaining this disequilibrium, the phases precipitated in the wake of such reaction front are at equilibrium. Therefore, the differences in the nagyágite response are indicative of several aspects of petrogenesis. The abundance of Te excess in nagyágite, as well as precipitation of native Te in the case of breakdown to galena-altaite, suggests that the pervading fluid was Te-rich. In the latter, the only modification shown by nagyágite is the one leading to Au-depletion. The resultant Au, from both depletion and breakdown processes, is removed from the areas of replacement, although slower infiltration rates assisted the precipitation of native Au in the halo that immediately surrounds the replaced nagyágite. Breakdown of nagyágite to galena-altaite symplectites is also reported to occur during remobilization processes at Sunrise Dam, W.A. (Sung et al., 2007). Here, the resulting Au is largely precipitated as native Au in the symplectites. Considering that the fluids are estimated at similar 300 °C in both deposits, the different behavior of Au infers that factors controlling Au solubility, such as pH, might differ in the pervading fluids. Otherwise, these fluids are quickly equilibrated to galena-altaite stability ($\log fS_2 = -10 \pm 1.5$ at 300 °C; Afifi et al., 1988), seen from the same type of molar-excess reaction. In turn, conditions conducive to the stable coexistence of galena and altaite are clearly not favorable to formation of nagyágite with normal, close to ideal composition. One can argue that destabilization of nagyágite occurs as a retrograde reaction during temperature decrease. In this case, however, the breakdown should be ubiquitous. This is not the case at Săcărîmb, and is more exception than rule. Secondly, the replacement should result in a marginal reaction rather than being cleavage-controlled.

Formation of Au-(Ag)-tellurides should be expected during nagyágite breakdown, given the availability of both Ag and Te (co-precipitation of hessite and native Te in the symplectites) although this is not observed. This may correlate with a higher fTe_2, above that at which Au-(Ag)-tellurides are stable, thus inhibiting their formation. Such reaction takes place in cases where Te is involved in additional substitutions (e.g., into the Me_2 site) during As-enrichment at the same time as Au-depletion occurs in the tiled areas. Differences in the availability of those elements involved at the reaction front, which impact on the behavior of Au, could be locally induced by variable reaction/infiltration rates even if the fluid has a uniform Te concentration. When the reaction is even faster (i.e., overgrowths of low-Pb nagyágite and hessite) a high-rate of Pb remobilization may also attract Te substitution into the Me_2 site; these reactions may inhibit substitution into the telluride layer even though Te is in excess. Re-precipitation of different varieties of nagyágite from the same parent lamella and the same type of molar deficit reaction can be explained by the buffering effect of co-precipitating phases. The latter provide for stabilization of one or the other nagyágite variety, if they have different chemistry (e.g., bournonite and altaite are hosts for low-Au or high-As varieties, respectively).

Positively charged Te is necessary for substitution into the Me_2 site (high-As and low-Pb varieties). This implies a higher oxidation state, which is typical for acidic fluids, as noted by Kovalenker et al. (1997) when addressing the occurrence of goldfieldite in a high-sulfidation environment. The same acidic character of overprinting fluids at Săcărîmb is inferred from the presence of goldfieldite and primary covellite in vein selvages (Ciobanu et al., 2005). An acidic fluid would be

strongly reactive to carbonates and may in turn trigger fluctuation in fTe_2/fS_2 across the stability fields of altaite and galena at 300 °C, thus providing conditions for nagyágite breakdown. Disequilibrium at this stage is also indicated by co-existence of minerals that are thermodynamically incompatible (e.g., Te-bearing löllingite, $[(Fe_{0.98}Ag_{0.01})_{\Sigma 0.99}(As_{1.71}Te_{0.20}S_{0.09}Se_{0.02})_{\Sigma 2.01}]$, and native tellurium; Ciobanu et al., 2004a). As seen from the ubiquitous carbonate halos around nagyágite, the resulting fluids react and further replace nagyágite after decomposition (breakdown products among the inclusions clustering the carbonate). At first, this is a molar deficit reaction, evidenced by jigsaw/sawtooth boundaries that indicate equilibrium interface to the parent nagyágite (Fig. 4a). This process evolves into replacement that is no longer driven by coupled dissolution-reprecipitation since the halos become irregular and include both native gold and tellurium (Fig. 4b), minerals that require 'jumps' in fTe_2 in order to precipitate within the same halo (see fTe_2/fS_2 stability diagrams; Afifi et al., 1988).

Considering the above, we suggest that the key factor that led to compositional variation in nagyágite at Săcărîmb is the variability in the local infiltration rates of pervading fluid rather than any significant differences in Te concentration. The variable infiltration rates for the fluids generated during the overprinting event can be caused by the relative position of those veins during reactivation involving rotation of the duplex system that controlled vein formation at Săcărîmb (Fig. 2). This event is obviously associated with a generation of fluids whose chemistry shared a higher acidity, but differed in the relative amounts of metals, due to factors such as local remobilization of pre-existing ores in each vein (e.g., As-richer in Nepomuc, Ag-richer in Margareta).

Conclusions

1. Nagyágite, with close to ideal composition, $Pb_3[Pb_{1.8}(Sb_{1.1},As_{0.1})_{\Sigma 1.2}]_{\Sigma 3}S_6(AuTe_2)$, and lamellar habit, formed during main-stage telluride mineralization at Săcărîmb and was a major component of the exploited ore. This is the 'normal' type of nagyágite.
2. Replacement *via* coupled dissolution-reprecipitation reactions is responsible for chemical variation in nagyágite at Săcărîmb, as documented from overprinting aspects in the veins on the western side of deposit; pseudomorphism is a key feature. This is likely to occur in any of the veins that were reactivated during rotation of the duplex-system responsible for vein formation.
3. Variable rates of molar excess reaction are associated with nagyágite breakdown to galena-altaite (faster) or galena replacement (slower). Molar deficit reaction leads to precipitation of nagyágite that has higher degrees of substitution by Sb + As for Pb in the Q modules.
4. What we call low-Pb nagyágite is also present in zoned platelets, outgrowing resorbed cores of ideal composition. Such platelets, strikingly different in habit to the normal type, are considered to form due to self-patterning in a residual precipitate that first led to crystallization of Ag-(Au)-tellurides. This process is likely to occur in precipitates of other compositions if nagyágite crystallization starts late and the system can be considered thermodynamically closed.

5. Slow reaction rate leads to a decrease in the Au content in nagyágite, in the presence of Te-bearing fluid, *via* Te → Au substitution. Diffusion assisted Au-depletion down to 0.7 apfu in normal nagyágite. Infiltration leads to precipitation of nagyágite that has a still more extensive decrease in Au content (0.3 apfu; low-Au); this involves a second substitution, of S for Te in the T layer.
6. The behavior of Au released during breakdown or depletion of nagyágite depends upon factors such as the infiltration rate, pH, fTe_2, etc. In molar-excess replacement, native gold is precipitated only at low infiltration rates (galena replacement); it is otherwise soluble in the pervading fluid and removed elsewhere. High fTe_2 precludes formation of Au-Ag tellurides even though Ag is available. Gold-depletion leads to formation of sylvanite when involvement of Te in additional substitutions (e.g., $Te \rightarrow Me_2$) provides for local decrease in fTe_2.
7. Destabilization of primary, 'normal' nagyágite is due to (i) high acidity of fluid (seen in the higher oxidation state required for $Te \rightarrow Me_2$ substitution) and (ii) changes in fTe_2/fS_2 within a narrow domain where altaite and galena coexist at 300 °C. The latter occurs when the host carbonate neutralizes the acidic fluid before interaction with nagyágite.
8. Nagyágite is a mineral with modular crystal chemistry and is able to adjust to variable rates of fluid infiltration by subtle chemical substitutions, as expressed by the general formula: $(Pb_3S_3)[(Pb_{2-x})(Sb,As,Te_b)_{1+x}]_{\Sigma 3}[(S_{3-y}Te_y)]_{\Sigma 3}(Au_{1-z-w}Te_{2+z}S_w)$, where $b = x + 1 - (Sb + As)$. Empirical values of b, x, y, z and w: $0 < b < 0.29$; $0.2 < x < 1.15$; $0 < y < 0.17$; $0 < z < 0.45$; $0 < w < 0.32$. The behavior of nagyágite, varieties thereof and any distinct, closely related compounds yet to be revealed, will map and assist coupling between dissolution and precipitation during such reactions.

Acknowledgements

We are grateful to the staff of Deva Gold S.A. for access to Săcărîmb and much discussion that has helped us appreciate the deposit. The comments and insight of journal reviewers Chris J. Stanley, Werner Paar, Herta Effenberger and F.J. Culetto are much appreciated, as is the editorial input of Associate Editor Paul Spry and Editor-in-Chief Johann Raith. CLC acknowledges receipt of an Australian Research Council 'Discovery' grant. We acknowledge the support of staff at the Adelaide Microscopy Centre, and especially Angus Netting, for assistance with calibration for numerous runs of electron probe microanalysis. NJC gratefully acknowledges facilities in Adelaide made available during his visits. This study is a contribution to International Geoscience Programme (IGCP) Project 486 'Au-Ag-Te-Se deposits'.

References

Afifi AM, Kelly WC, Essene EJ (1988) Phase relations among tellurides, sulfides, and oxides: II. Application to telluride-bearing ore deposits. Econ Geol 83: 395–404

Alderton DHM, Fallick AE (2000) The nature and genesis of gold-silver-tellurium mineralization in the Metaliferi Mountains of western Romania. Econ Geol 95: 495–515

Alderton DHM, Simon G, Ioan M, Panazan I, Orlandea E, Csibi I (1997) Geochemical studies of gold-silver-tellurium mineralization in the vicinity of Sacaramb, Southern Apuseni Mountains, Romania: Some preliminary results. Rom J Mineral 78: 31–38

Bengel H, Jobic S, Moelo Y, Lafond A, Rouxel J, Seo DK, Whangbo MH (2000) Distribution of the Pb and Sb atoms in the (Pb,Sb)S layers of the franckeite-type misfit compound $[(Pb,Sb)S]_{2.28}NbS_2$ examined by scanning tunneling and atomic force microscopy. J Solid State Chem 149: 370–377

Berbeleac I, Popa T, Ioan M, Iliescu D, Costea C (1995) Main characteristics of Neogene-volcanic-subvolcanic structures and hosted ore deposits in Metalliferi Mountains. Geol Macedonica 9: 51–60

Bindi L, Cipriani C (2004) Museumite, $[Pb_2(Pb,Sb)S_8](Te,Au)_2$, a new mineral from the gold-telluride deposit of Săcărîmb, Metaliferi Mountains, western Romania. Eur J Mineral 16: 835–838

Brese NE, O'Keeffe M (1991) Bond-valence parameters for solids. Acta Cryst B47: 192–197

Cabri LJ (1965) Phase relations in the Au-Ag-Te system and their mineralogical significance. Econ Geol 60: 1569–1606

Ciobanu CL, Cook NJ, Damian G, Damian F, Buia G (2004a) Telluride and sulphosalt associations at Săcărîmb: In: Gold-Silver-Telluride deposits of the Golden Quadrilateral, South Apuseni Mts., Romania. IAGOD Guidebook Series, Vol. 12, pp 145–186

Ciobanu CL, Găbudeanu B, Cook NJ (2004b) Neogene ore deposits and metallogeny of the Golden Quadrilateral, South Apuseni Mountains, Romania: In: Gold-Silver-Telluride deposits of the Golden Quadrilateral, South Apuseni Mts., Romania. IAGOD Guidebook Series, Vol. 12, pp 25–88

Ciobanu CL, Cook NJ, Căpraru N, Damian G, Cristea P (2005) Mineral assemblages from the vein salband at Săcărîmb, Golden Quadrilateral, Romania: I. Sulphosalts. Geochem Mineral Petrol 43: 47–55

Cioflica G, Jude R, Lupulescu M, Simon G, Damian G (1993a) New data on the tellurides of the Neogene ore deposits in Romania. Rom J Mineral 76 [Suppl 1]: 11–12

Cioflica G, Jude R, Lupulescu M, Simon G, Damian G (1993b) The tellurides of the Romanian Neogene ore deposits. In: Fenoll Hach-Ali P, Torres-Ruiz T, Gervilla F (eds) Current research in geology applied to ore deposits. Proc. 2nd Biennial SGA Meeting, Granada, Spain, September 1993, pp 73–76

Cook NJ, Ciobanu CL (2005) Tellurides in Au deposits: implications for modelling. In: Mao JW, Bierlein FP (eds) Mineral deposit research: Meeting the global challenge, Springer, Berlin, pp 1387–1390

Cook NJ, Ciobanu CL, Damian CL, Damian F (2004) Tellurides and sulphosalts from deposits in the Golden Quadrilateral. In: Gold-Silver-Telluride deposits of the Golden Quadrilateral, South Apuseni Mts., Romania. IAGOD Guidebook Series 12, pp 111–144

Cook NJ, Ciobanu CL, Căpraru N, Damian G, Cristea P (2005) Mineral assemblages from the vein salband at Săcărîmb, Golden Quadrilateral, Romania: II. Tellurides. Geochem Mineral Petrol 43: 56–63

Cooke DR, McPhail DC (2002) Epithermal Au-Ag-Te mineralization, Acupan, Baguio District, Philippines; numerical simulations of mineral deposition. Econ Geol 96: 109–131

Căpraru N (2004) New interpretations of the structure of the Săcărîmb project area. In: Gold-Silver-Telluride deposits of the Golden Quadrilateral, South Apuseni Mts., Romania. IAGOD Guidebook Series, Vol. 12, 218 pp

Drew LJ (2003) Model of the porphyry copper and polymetallic vein family of deposits – applications in Slovakia, Hungary, and Romania. Internat Geol Rev 45: 143–156

Eckel EB (1997) Minerals of Colorado. Fulcrum Publishing, 676 pp

Effenberger H, Paar WH, Topa D, Culetto FJ, Giester G (1999) Towards the crystal structure of nagyágite, $[Pb(Pb,Sb)S_2]$ (Au,Te). Amer Mineral 84: 669–676

Effenberger H, Culetto FJ, Topa D, Paar WH (2000) The crystal structure of synthetic buckhornite, $[Pb(Pb,Sb)S_2][(Au,Te_2)]$. Z Krist 215: 10–16

Gál A, Molnár F, Ghergari L, Szabó C, Gatter I (2003) Fluid inclusions and morphology of quartz from the Neogene epithermal deposits, Brad-Săcărîmb area (Transylvania, Romania). Stud Univ Babeş-Bolyai Cluj-Napoca, Ser Geol Special issue 2003: 40–41

Ghiţulescu TP, Socolescu M (1941) Étude géologique et minière des Monts Metallilifères (Quadrilatère aurifère et régions environnantes). Anarul Inst Geol 21: 181–464

Giuşcă D (1935) Note preliminaire sur la genèse du gisement aurifère de Săcărîmb. Bul Lab Min Gen Univ Bucuresti 1: 72–82

Giuşcă D (1936a) La genèse du gisement aurifère de Săcărîmb. CR Acad Sci Roum 1: 243–246

Giuşcă D (1936b) Nouvelles observations sur la minéralisation des filons aurifères de Săcărîmb (Nagyag). Bull Acad Roum Sci 18: 3–5; 97–103

Giuşcă D (1937) Le chemisme de la nagyágite. Bul Soc Roum Geol 3: 118–121

Gossner B (1935) Über Kristallform und molekulare Einheit von Nagyagit. Zentralbl Mineral: 321–327

Haidinger W (1845) Handbuch zum Bestimmen von Mineralien. Braunmüller und Siedel, Vienna, 556 pp

Hankó W (1888) Chemical analysis of sylvanite and nagyágite from Nagyag. Math t-t. Ért. 6: 340–349 (in Hungarian)

Helke A (1934) Die Goldtellurerzlagerstätten von Săcărîmb (Nagyag) in Rumänien. N Jb Mineral Geol Palaeontol Abh, Abt A (Mineral, Petrogr) 1: 19–85

Ianovici V, Borcoş M, Bleahu M, Patruliu D, Lupu M, Dimitrescu R, Savu H (1976) Geologia Munţilor Apuseni. Ed Acad Rep Soc România, Bucureşti, 631 pp

Jensen EP, Barton MD (2000) Gold deposits related to alkaline magmatism. Rev Econ Geol 13: 279–314

Kovalenker VA, Safonov YG, Naumov VB, Rusimov VL (1997) Epithermal gold-telluride deposits of Kochbulak (Uzbekistan). Geol Ore Deposits 39: 127–152

Lafond A, Nader A, Moëlo Y, Meerschaut A, Briggs A, Perrin S, Monceau P, Rouxel J (1997) X-ray structure determination and superconductivity of a new layered misfit compound with franckeite-like stacking $[(Pb,Sb)S]_{2.28}NbS_2$. J Alloys Compounds 261: 114–122

Lupulescu M (1997) Nagyágite: New data and considerations. Rev Roum Geol 41: 29–36

Makovicky E (1993) Rod-based sulphosalt structures derived from SnS and PbS archetypes. Eur J Mineral 5: 545–591

Markham NL (1960) Synthetic and natural phases in the system Au-Ag-Te. Econ Geol 55: 1148–1178 & 1460–1477

Ortoleva PJ (1994) Geochemical self-organization. Oxford Monographs in Geol, Geophys 23, 411 pp

Paar WH, Chen TT (1982) Tellurides in ores from the Schellgaden gold deposit and from the Katschberg-north tunnel (in German). Der Karinthin 87: 371–381

Pálfy M (1912) Geologische Verhältnisse und Erzgänge des Siebenbürgischen Erzgebirges. Jahrbuch der kaiserlich-königlichen ungarischen geologischen Anstalt Budapest, 17 (45): 4 pp

Papp G (2004) History of minerals, rocks and fossil resins discovered in the Carpathian region. Studia Naturalia 15. Hungarian Nat Hist Museum, Budapest: 215 pp

Putnis A (2002) Mineral replacement reactions: from macroscopic observations to microscopic mechanisms. Mineral Mag 66: 689–708

Putnis CV (2006) Texture development in coupled dissolution-reprecipitation replacement reactions. 19th General Meeting of the Int. Mineral Assoc., Kobe, Japan, Program & Abstracts, 173 pp

Schrauf A (1878) Über die Tellurerze Siebenbürgens (Silvanit, Krennerit, Nagyagit, Hessit, (Petzit). Z Krist Min 2: 209–252

Scopoli GA (1769–1772) Principia mineralogiae systematicae et practicae. Prague

Shimizu M, Shimizu M, Cioflica G, Shimazaki H, Kovacs M, Lupulescu M, Petruşan G, Feigel M, Popa G, Refec I, Pânzan I (1999) New informations on opaque minerals from Neogene ore deposits in Romania. International Symposium 'Mineralogy in the System of Earth Sciences', Abstr vol, Univ Bucharest, 101 pp

Shimizu M, Stanley CJ (2003) Re-study of nagyágite from Sacarimb, Romania. In: Eliopoulos DG et al (eds) Mineral exploration and sustainable development. Millpress, Rotterdam, pp 527–528

Şimon G, Alderton DHM (1995) Pilsenite, Bi_4Te_3 from the Săcărîmb gold-telluride deposit, Metaliferi Mts.; first occurrence in Romania. Rom J Mineral 76 [Suppl 2]: 111–113

Şimon G, Alderton DHM, Bleser T (1994) Arsenian nagyágite from Săcărîmb, Romania: a possible new mineral species. Mineral Mag 58: 473–478

Sipöcz L (1885) Über die chemische Zusammensetzung einiger seltener Minerale aus Ungarn. Z Krist 11: 209–219

Spiridonov EM (1991) Nagyagit $AuPb_5Te_{4-x}Sb_xS_6$, $x = 0$–2. Novyye Dannyye o mineral SSSR 37: 128–138 (in Russian)

Stanley CJ, Roberts AC, Harris DC (1994) New data for nagyágite. Mineral Mag 58: 479–482

Stumpfl EF (1970) New electron probe and optical data on gold tellurides. Am Mineral 55: 808–814

Sung Y-H, Ciobanu CL, Pring A, Brügger J, Skinner W, Cook NJ, Nugus M (2007) Tellurides from Sunrise Dam gold deposit, Yilgarn Craton, Western Australia: a new occurrence of nagyagite. Mineral Petrol 91: 249–270

Tenailleau C, Pring A, Etschmann B, Brügger J, Grguric BA, Putnis A (2006) Transformation of pentlandite to violarite under mild hydrothermal conditions. Am Mineral 91: 706–709

Udubaşa G (1986) Parageneses of some opaque minerals in rocks and ores. In: Craig JR et al. (eds) Mineral parageneses. Theophrastus Publ., Athens, pp 55–74

Udubaşa G, Strusievicz RO, Dafin E, Verdeş G (1992) Mineral occurrences in the Metaliferi Mts., Romania. Rom J Mineral 75 [Suppl 2]: 1–35

Udubaşa G, Wagner F, Friedl J (1993) Nagyágite: Some features of its composition and Mossbauer spectra. Rom J Mineral 76 [Suppl 1]: 50

View publication stats